Final Draft
of the original manuscript:

Nwaogu, U.C.; Blawert, C.; Scharnagl, N.; Dietzel, W.; Kainer, K.U.:
Effects of organic acid pickling on the corrosion resistance of magnesium alloy AZ31 sheet
In: Corrosion Science (2010) Elsevier

DOI: 10.1016/j.corsci.2010.03.002

Effects of organic acid pickling on the corrosion resistance of magnesium alloy AZ31 sheet.

U. C. Nwaogu[a]*, C. Blawert[b]*, N. Scharnagl[b], W. Dietzel[b], K. U. Kainer[b]

[a]Technical University of Denmark

Department of Mechanical Engineering

Building 425,

DK – 2800 Kgs. Lyngby

Denmark.

[b]Institute of Materials Research

GKSS-Forschungszentrum Geesthacht GmbH

D-21502 Geesthacht, Germany

***Corresponding authors:** ugon@mek.dtu.dk (U. C. Nwaogu),
carsten.blawert@gkss.de (C. Blawert)

Abstract

Organic acids were used to clean AZ31 magnesium alloy sheet and the effect of the cleaning processes on the surface condition and corrosion performance of the alloy was investigated. Organic acid cleanings reduced the surface impurities and enhanced the corrosion resistance. Removal of at least 4 µm of the contaminated surface was required to reach corrosion rates less than 1 mm/year in salt spray condition. Among the three organic acids examined, acetic acid is the best choice. Oxalic acid can be an alternative while citric acid is not suitable for cleaning AZ31 sheet, because of insufficient removal of iron impurities.

Keywords: A. Mg alloy; A. Acid solutions; C. Pitting corrosion; B. Weight loss; B. IR spectroscopy; B. EIS.

1. Introduction

Mg alloys have many desirable properties such as low density, high strength to weight ratio, ease of castability, weldability, machinability and recyclability [1,2]. The combination of these properties leads to an increasing use in various areas such as electronic, automobile and aerospace industries [3,4] where light weight materials are required to reduce weight while simultaneously reducing fuel consumption and subsequent green house gas emissions [5]. However, Mg alloys are susceptible to corrosion attack and this has limited the wide-spread application. The major challenge is the protection of these alloys from corrosion attack. The impurity metal elements such as Ni, Fe and Cu and heavy metal containing intermetallic phases form micro-galvanic couples with the alloy matrix [1]. The deleterious effects of these elements are due to their low-solid solubility limits and their ability to serve as active cathodic sites for the reduction of water at the sacrifice of elemental magnesium [6]. Corrosion can be minimized by the use of high purity alloys that maintain metal impurities below the tolerance limits. The removal of bad design, flux inclusions, surface contaminations, galvanic couples and inadequate or incorrectly applied surface protection schemes can also significantly decrease the corrosion of Mg alloys in service [1]. However, thermo-mechanical processing of these alloys may lead to an increase of the surface impurity content above the tolerance limits. To this end the surfaces of Mg alloys are supposed to be pre-cleaned before further surface modification to enhance their corrosion resistance and surface appearance [7]. Mechanical and chemical cleaning methods or combinations of both can be used depending on the specific application and product involved [8]. For this study, chemical cleaning processes with organic acids were used. Acid cleaning is a useful method for the removal of contaminations, such as natural oxide tarnish, embedded sand or heavy metal impurities and burned-in lubricants that are tightly bound to the surface or insoluble in solvents and alkaline solutions. In addition to the cleaning effect of acid pre-treatment, an anti-corrosive effect can be obtained by the formation of protective layers on the surface of the magnesium alloys by some acids [9]. The efficiency of the cleaning processes can be tested by evaluating the corrosion rate in contact with NaCl solution, because magnesium alloys without any surface contamination exhibit lower corrosion rate than contaminated surfaces [9]. Most of the acid cleanings for

Mg alloys found in literature have been done with inorganic acids such as chromic, phosphoric, hydrochloric, hydrofluoric and nitric acids with various concentrations and not much is reported for organic acids. One of the few studies based on organic acid (acetic acid) is the investigation by R. Supplit [10], on the anti-corrosive effect of acid pickling and sol-gel coatings on AZ31 Mg alloy. The results showed that acid pickling reduces corrosion of AZ31 Mg alloy significantly, while acetic acid removed more material from the surface of the cleaned specimen and produced better corrosion resistance. However, our own work on inorganic acids [11] has indicated that the cleaning efficiency of various acids (phosphoric, nitric and sulphuric acids) and the corrosion protection mechanisms were remarkably different, thus it would be interesting to check whether the same can be observed for organic acids. The organic acids used for this investigation include acetic, oxalic and citric acids. Acetic acid was selected based on available information in literature [8]. No previous work or literature was found for oxalic and citric acids. They were chosen for this study to access their potential in pickling of Mg alloy sheet, because they form soluble salts with iron as the main impurity.

2. Experimental

The material investigated is a commercial magnesium alloy AZ31 sheet of 2 mm thickness (as-received; AR) with chemical composition given in Table 1. From Table 1, it can be seen that the surface is contaminated with iron and nickel from the rolling of this alloy sheet. The sheet was press-cut into two sets of specimens of dimensions 50 mm x 50 mm x 2 mm and 50 mm x 20 mm x 2 mm using Durma MS 2004 Plate shear. A solution of NaOH for alkaline degreasing of the surfaces and three concentrations of each of the acids were prepared in the concentrations given in Table 2. The medium concentrations and cleaning times were chosen according to the information obtained from literature [8] for acetic acid. Higher and lower concentrations as well as longer and shorter cleaning times were selected accordingly. For oxalic and citric acids, several tests were performed before the concentrations were chosen. Therefore, the selected concentrations for each acid differ. The presence of $Ca(NO_3)_2$ in the later solutions had little effect so that it was not used.

The cleaning process was started by dipping the specimen in 1 M solution of NaOH for 60 s to degrease the plates (alkaline cleaning). After the alkaline cleaning, the plates were rinsed in deionized water and dried in a warm stream of air at a temperature slightly above room temperature. Then, the acid pickling was performed. After dipping, the specimens were rinsed in deionized water and acetone and dried in a warm stream of air accordingly. The composition of the cleaning solutions and the cleaning conditions are provided in Table 2. The specimens (50 mm x 50 mm x 2 mm) for the salt spray test were weighed before and after cleaning using a Mettler AC 100 electronic balance and the weights were recorded. The difference in weight before and after cleaning (weight loss) gave the material removed in micrometer (μm) as calculated from equation (1) below.

$$W = \frac{w \times 10^4}{\rho \times A} \qquad (1)$$

where W = material removed in μm

w = weight loss in g

ρ = density in g/cm^3

A = area in cm^2

10^4 = a unit conversion factor.

Considering the large number of specimens investigated, a corrosion screening test was performed based on salt spray testing (SST) EN ISO 9227. The as-received and cleaned specimens were exposed to fog formed from neutral 5 % NaCl solution in a Weiss SC 450 salt spray chamber for a period of 48 hours. The corrosion rates (mm/year) in salt spray test were evaluated using equation 2.

$$R = \frac{8.7757 \times 10^4 \times w}{\rho \times A \times t} \qquad (2)$$

where R = corrosion rate in mm/year in salt spray test

t = time in hours

8.7757×10^4 = used for unit conversion.

The specimens with dimensions 50 mm x 20 mm x 2 mm were subjected to surface characterisation. A Hommel T1000 contact profilometer was used to determine the surface roughness (R_a-parameter) of the as-received and cleaned specimens. A SPECTROLAB

spark discharge optical emission spectroscopy device (SD-OES) with spark analyzer vision software was used to determine the average elemental compositions on the surfaces of as-received and cleaned specimens. The elemental composition obtained is the average of three different runs for each specimen analysing from the surface down to a depth of approximately 100 μm. This implies that the measured elemental composition is only an average over this depth and the real surface contamination is even higher (about 20 times assuming 5 μm depth of severely contaminated surface). Due to the heavy deformation during rolling the contamination is not only restricted to the top surface, thus especially enrichment of heavy metal impurities can be seen, even if they are "diluted" by the larger analyzed volume.

To extend the understanding of the mechanisms of cleaning and improved corrosion resistance, the best and the worst conditions for each acid were selected for further characterization. The best and worst treatments are defined by the lowest and highest corrosion rates obtained for each acid from SST.

The surface morphology and the elemental composition were examined in a ZEISS Ultra 55 scanning electron microscope (SEM) coupled with Energy Dispersive X-ray Spectroscopy (EDX) detector at an accelerating voltage of 15 kV. Additional information about the phases and compounds on the surface of the selected specimens was obtained with an infrared (IR) spectrometer Bruker Tensor 27 with Opus software. Further corrosion investigations were performed using electrochemical impedance spectroscopy (EIS). A typical three electrode cell with 300 ml of neutral 5 % NaCl electrolyte, a platinum mesh as counter electrode, Ag/AgCl reference electrode and the specimens of AZ31 alloy as the working electrode was used. The EIS measurements were performed at open circuit potential over a frequency range from 10 kHz to 0.01 Hz with a potential amplitude signal of 10 mV after 2 and 20 hours of immersion in the electrolyte respectively, using a Gill AC potentiostat.

3. Results

3.1 Material removal

The variation of material removed with immersion time for different concentrations of acetic, oxalic and citric acids is presented in Fig. 1. The amount of material removed increases with time and concentration for all acids, only with one exception in the case of the treatment with 80 g/l oxalic acid and 120 s immersion time. By changing the acid, the concentration and immersion time; material removal can be adjusted from 1 to 20 μm. Acetic and citric acids gave the highest material removal (21.23 μm and 15.50 μm respectively) for their highest concentrations (300 g/l and 120 g/l respectively) after 120 s. The result obtained for acetic acid is consistent with the result reported in [10]. All concentrations of oxalic acid showed similar trend except its highest concentration (80 g/l). A consideration of the cleaning rates, Fig. 2, shows that the cleaning rates increased with increasing concentrations of each acid at each immersion time. For acetic acid cleaning rates from 4 to 10 μm/min were measured with increasing concentration. For oxalic acid the concentration influence was more extreme and the corrosion rates were found to be between 2 and 18 μm/min. The lowest influence was finally determined for citric acid with rates between 2 and 7 μm/min. However, a strong influence of the immersion time on the overall cleaning rate was detected as well for specimens cleaned in solutions of the same concentration. For most of the specimens the rate is decreasing with increasing immersion time, but there are a few exceptions. The cleaning rates of acetic acid for the lower concentration decreased steadily but for the high concentration there was a decrease followed by an increase at longer immersion time. The cleaning rate for citric acid was rather stable unlike that of oxalic acid which decreased with immersion time with strong decrease for the highest concentration. The observed features are attributable to the various concentrations of each acid determining the interaction with the surface.

3.2 Surface appearance and roughness

The AZ31 magnesium alloy after cleaning in acetic or citric acids had a greyish surface appearance. The use of oxalic acid resulted in a brown spotted surface appearance with some loose dusty deposition products. The pickling has a clear effect on the surface

roughness. Fig. 3 shows that the R_a values of the surfaces of the specimens cleaned in the three acids depended on the amount of material removed. For comparison the R_a values of the as-received specimens are also shown. It is interesting to see that with material removal of less than or equal to 5 μm, the R_a values were reduced compared to that of the as-received material. However, above 5 μm material removal, the R_a values of treated specimens increased rapidly. The increase is largest for oxalic acid followed by citric acid and then acetic acid. This could probably be attributed to the effect of the $Ca(NO_3)_2$ in acetic acid making the material removal more uniform. However, this assumption has to be checked in further studies.

3.3 Surface impurity level

The impurity level measured in the bulk and on the surface of the as-received specimens of the commercial AZ31 Mg alloy sheet by SD-OES (Table 1) clearly shows that the main impurities of concern are Fe and Ni. The copper content in both locations is comparable; therefore the Cu impurity level is negligible in this case. It is expected that with surface material removal, the concentration of impurities on the surface of the alloy will be reduced. The variation of the impurity level for each of these elements relative to the material removed is presented in Fig. 4 for each acid. Fig. 4a shows that the surface of the as-received specimen has a slightly higher copper impurity level than the bulk surface composition. The acetic and oxalic acid cleaning revealed a comparable copper composition with the bulk if sufficient material is removed. It is also evident that some conditions of treatment with oxalic and citric acids showed higher level of copper impurity relative to the as-received specimen. Fig. 4b presents the iron impurity level against the material removed. It can be seen from this figure that there is a significant reduction of the impurity level for all the treated specimens relative to the as-received specimen. It is seen that only specimens treated in acetic and oxalic acids showed iron impurity level lower than the standard composition and comparable to the bulk composition if at least 5 μm of material is removed. Acetic, oxalic and citric acids form soluble organo-metal complexes with iron and remove iron from the surface by this means. In spite of this, the citric acid treatment showed iron impurity level more than 50 ppm even if more than 5 μm material is

removed. The nickel impurity level for most of the acids is well below the standard nickel impurity composition (Fig. 4c). Removal of Ni appears to be successful with all three acids. From Fig. 4, considering all impurities, it is seen that acetic and oxalic acids reached comparable impurity level as the bulk with up to 4 μm material removal while citric acid only reached the standard composition after around 5 μm material removal. However, both levels of material removal would be sufficient to guarantee good corrosion resistance.

3.4 Salt spray test (SST)

The variation of the corrosion rates in salt spray test obtained as a function of material removed for the specimens cleaned in the three acids are shown in Fig. 5. It can be seen that the corrosion rates were significantly reduced after cleaning in all the acids as material removal increases. This suggests that the cleaning processes were effective in the removal of the surface contaminants and metal impurities that are deleterious to the corrosion behaviour of AZ31 magnesium alloys. This is consistent with the measured surface impurity levels. Fig. 5 shows that specimens cleaned in acetic acid reveal the lowest corrosion rates without any fluctuations in the corrosion rate if more than 4 μm are removed. This is because the metal surface was heavily etched and this also reflected on the amount of material removed from the surface of these specimens. However, it is obvious that for the other two acids 4 μm of material removal is also sufficient but some fluctuations in the corrosion performance are still visible. Most of the oxalic acid treatments reached corrosion rates of about 1 mm/year whereas for citric acid, the corrosion rates are closer to 2 mm/year.

To understand the cleaning mechanisms as well as the influence of the different acids on the surface condition of the alloy and the corrosion resistance, a detailed microstructural investigation was carried out on the best (lowest corrosion rate) and worst (highest corrosion rate) conditions in SST. The conditions of treatment (concentrations and immersion times), the material removed, corrosion rates and the impurity level for the selected specimens are presented in Tables 4 and 5 for best and worst conditions respectively. For acetic acid, the highest material removal of 21.23 ± 1.52 μm gave rise to

the lowest impurity level leading to the lowest corrosion rate of 0.34 ± 0.04 mm/year as presented in Table 4. Oxalic acid followed with a corrosion rate of 0.59 ± 0.11 mm/year obtained from an intermediate surface impurity level as a result of material removal of 8.41 ± 1.01 µm from the surface of the specimen. Finally, for citric acid, a corresponding impurity level obtained from 4.33 ± 0.28 µm material removal lead to a corrosion rate of 0.72 ± 0.07 mm/year as shown in Table 4. From Table 5, the worst corrosion behaviour was observed for oxalic acid treated specimen with a material removal of 0.58 ± 0.06 µm. This implies that the impurity level on this specimen is very high as less material is removed leading to a corrosion rate of 9.48 ± 0.22 mm/year. This is followed by citric acid treated specimen with a material removal of 0.65 ± 0.08 µm leading to a corresponding corrosion rate of 5.96 ± 0.81 mm/year and finally, acetic acid treated specimens with a material removal of 2.09 ± 0.18 µm giving a corrosion rate of 5.38 ± 0.80 mm/year. From Table 4 and 5 it is obvious that the amount of material removed is the parameter that has the strongest influence on the impurity levels and thus on the corresponding corrosion rates in SST. The more material is removed from the surface of the specimens, the lower the surface impurity level and the higher the corrosion resistance.

3.5 Surface morphology

The micrographs of the as-received specimen and the treated specimens (with best and worst conditions in SST) for each acid are presented in Figs. 6 and 7 respectively. A closer look at the surface morphologies of the treated specimens showed a significant contrast to the as-received specimen. There has been an evident material removal from the surface of the treated specimens. The scratches indicating the rolling direction are not visible anymore on the surface of the treated specimens with best conditions and while they are still visible on the surfaces of the specimens with the worst conditions. This indicates that there is only effective material removal for the best conditions. It means that the impurity level of these specimens can be expected to be significantly reduced by the acid cleaning as compared to the as-received specimen or the worst cleaning conditions.

A detailed examination of the micrographs of the treated specimens (Fig. 7) was performed for the best and worst conditions for each of the acids. The specimen cleaned in acetic acid revealed the grains and grain boundaries of the substrate (Fig. 7a). This is a clear indication of the effective etching reflecting in the high material removal. For the worst condition, it is evident that the matrix around the impurities has been removed by the acid cleaning but the impurities were not removed due to the shorter immersion time (Fig. 7b). However, with longer immersion time the impurities were completely removed as can be seen form Fig. 7a. There is no evidence of film formation on the surface of the substrates. The etching in oxalic acid was more homogeneous and shows the grain boundaries if the cleaning is successful (Fig. 7c). Surface contaminants are still present on the surface after poor cleaning and the grain structure is not developed (Fig. 7d). There is also no evident film formation on the surface of the specimens. The surface of specimens treated with citric acid shows only uniformly distributed pits on the surface without the development of the grains (Fig. 7e). For the worst condition, the etching was clearly not sufficient to remove the severely deformed surface region and the lines of rolling direction of the sheet are still visible (Fig.7f) indicating that not enough material was removed. All the results indicate that the highly deformed and contaminated surface has to be completely removed for good corrosion resistance. Only if sufficient material has been removed the globular grain structure was visible and a good corrosion resistance can be expected.

3.6 Surface phases and elemental composition

The infrared spectra of the surfaces of as-received specimen and specimens treated in different acids with the best corrosion behaviour (best conditions) in SST are presented in Fig. 8. From the figure, it can be seen that the spectra of cleaned specimens (Fig. 8b-d) have similar bands as present in the spectrum of as-received specimen (Fig. 8a). The bands similarity in the spectra is characteristic of a series of closely related (iso-structural) compounds [12]. In addition, the spectra of the cleaned specimens show bands emanating from the products (salts) of the reaction of the acids with the substrate elements. The compounds present on the surface according to the acid used include acetates, oxalates or citrates of the major divalent and trivalent metals (Table 3). Their oxides and hydroxides

are also present but at a lower level. However, the concentration of hydroxide after cleaning in citric acid is high (Fig. 8d). There is also presence of carbon dioxide (CO_2) gas which probably was due to adsorption of the atmospheric carbon dioxide on the surface of the substrate. Some of these CO_2 will react with moisture to form carbonates on the surface of the specimens. The presence of acid anions on the surface of the cleaned specimens as reaction products (salts) is due to the reactions between the substrate elements and the acids. From the IR results, the oxides, hydroxides, carbonates and acetates, oxalates or citrates of the base, alloying and impurity elements are detected on the surfaces of the treated specimens depending on the acid used.

The results of the EDX point analyses for elemental composition of the surfaces of the as-received and treated specimens with best condition for each acid are shown in Table 6. Fig. 9 illustrates the locations of the analyses. Considering the elemental composition of the matrix in all the cases, it is seen that there is no evidence for surface film formation. This is also in agreement with the surface morphology presented in Fig. 7, for the best conditions. For the other points, it can be seen that they mainly contain the alloying elements and the base metal and some oxides of the alloying elements and the base metal. The only impurity element present in one of the points on acetic acid cleaned specimen is Fe (0.28 %). This was not observed for any points analysed for oxalic acid cleaned specimen. A low amount of Fe (0.11 %) was found in the matrix of citric acid cleaned specimen and in one of the points (1.21 %) as shown in Table 6. Furthermore, the elemental compositions correlate with the expected standard of AZ31, only the surface treated with citric acid showed presence of Na of which the source is not known. There is also presence of carbon in almost all the points on citric acid cleaned surface except in the matrix. This could be attributed to insoluble citrates of Zn or carbonates as shown by the high absorbance peak of these anions in the IR spectrum (Fig. 8d). However, there are also other visible phases on the surfaces of the specimens. Impurities such as pure iron, iron oxides, copper and iron enriched particle and carbon rich debris were still visible on the surfaces of the as-received specimen. From Table 6, it is clear that after cleaning these impurities were drastically

reduced for the specimens treated with acetic and oxalic acids. Citric acid treated specimen still has significant amount of Fe present.

3.7 Tolerable surface impurity level

The impurities were not completely removed therefore, it will be reasonable to identify tolerable impurity levels that can guarantee sufficiently high corrosion resistance (i.e. corrosion rate less than 1 mm/year). The impurity levels from SD-OES for best and worst condition for each acid are shown in Fig. 10. The impurity level after pickling is compared with the impurity content on the surface (AR) and in the bulk (after grinding off 500 μm of as-received specimen) representing the maximum and minimum impurity level of AZ31 Mg alloy. It became clear that there are significant reductions in the impurity level of Fe and Ni for the selected specimens with best corrosion behaviour in SST compared to the as-received specimen (Fig. 10a). It can be seen that acetic and oxalic acid treated specimens reached the bulk impurity level unlike citric acid which still showed very high amount of Fe on the surface. This is consistent with the result of EDX point analysis. This behaviour might put an impediment on the use of citric acid as a cleaning solution for Mg alloys. From Fig. 10a, the impurity level to guarantee sufficient corrosion resistance can be identified as being < 20 ppm for Fe, and < 10 ppm for Ni. However, these values are average values taken from a depth down to 100 μm from the top surface as a consequence, values obtained closer to the surface, i.e. < 100 μm, might be higher. This low impurity level with the corresponding low corrosion rates is only obtained with acetic and oxalic acids. It is also evident in Fig. 10a that cleaning has almost no effect on the copper impurity level. Overall, cleaning with acetic and oxalic acids is more effective in the reduction of the surface impurity level than citric acid. For the worst conditions, the results shown in Fig. 10b reveal that in spite of some material removal the amount was not sufficient to reach the standard impurity levels. Only acetic acid has approached this level, but even at this level the corrosion rates are still high.

3.8 Electrochemical impedance spectroscopy results

The electrochemical impedance spectroscopy results of the as-received specimen and specimens with best performance in SST are presented in Fig. 11. The measurements were performed after 2 and 20 hours of exposure to neutral 5 % NaCl solutions. All the specimens showed only one capacitive loop in the high frequency region, which indicates the same corrosion mechanism for all specimens [13 – 16]. The figure also revealed that all the plots have a low frequency region with negative values of the imaginary impedance. This region is the inductive loop which is attributed to the relaxation of adsorbed species [16, 17,] such as $Mg(OH)^{+}$ or $Mg(OH)_2$ [17]. According to M. Anik and Celikten [17], the adsorption of these species is only significant in the absence of protective oxide layer.

The diameter of the capacitive loop is associated with the charge-transfer resistance (R_p) and subsequently, with the corrosion resistance [18, 19]. Therefore, the higher the charge transfer resistance, the better the corrosion resistance. From Fig. 11, the specimens showed increased R_p values with immersion time indicating a decrease of the corrosion rate. Considering Fig. 11a, acetic acid showed higher resistance values (R_p) than the specimens treated with the other acids. This is attributed to the extent of material removal. It is also clear that specimens cleaned in oxalic and citric acid also showed higher R_p values than that of the as-received specimen. From Fig. 11b, it can be seen that there is significant improvement in the impedance values after 20 hours immersion in the corrosive solution for all specimens. However, acetic acid treated specimen still showed the highest R_p value, although the other specimens showed enhanced corrosion resistance as well. The as-received specimen still revealed the lowest R_p value. This confirms that surface impurities contributed significantly to the degradation of the corrosion resistance of AZ31 Mg alloy.

4. Discussion

The primary goal of this study is the reduction of surface impurities to enhance the surface corrosion resistance of magnesium alloy AZ31 sheet. The source of the contamination is from the rolling process where the alloy surface is deeply enriched with iron and nickel. The copper impurity level of the studied AZ31 alloy is low and therefore not a threat to the corrosion resistance. It is intended to find out more environmentally friendly and cost

effective cleaning solutions for AZ 31 magnesium alloy which could replace the cleaning solutions that are not environmentally friendly for example solutions containing hexavalent chromium ion [8]. Our previous studies [11] showed that the surface is mainly contaminated with heavy metal particles, intermetallics and carbon-rich debris, which have to be eliminated or reduced in order to achieve the aim. Material removal is a question of cost and compromise to dimensional precision as a result care must be taken in heavy etching.

As reported in [11] for inorganic acid based cleaning solutions, their organic counterparts can also remove up to 5 μm or more from the surface of the AZ31 alloy sheet within 1 min of cleaning operation depending on the concentrations. However, for the current study, 4 μm represents the minimum amount of removed material that can guarantee a significant corrosion resistance in salt spray corrosion behaviour. However, there are distinct differences in the cleaning effectiveness and mechanisms between the three organic acids. This will be discussed in detail below.

Considering the initial cleaning rates, the highest can be obtained for oxalic acid with an average cleaning rate of 18.70 μm/min within the first 15 s, while acetic and citric acids have average cleaning rates of 10 and 6.5 μm/min, respectively. This trend follows the effective hydrogen ion (H^+) concentrations (pH values) for the acids (1.29, 1.84 and 2.00 for oxalic, acetic and citric acids respectively). The pH is not directly related to the concentrations of the acids because they are not completely dissociated (organic acids are weak acids). However, the more acidic the solution, the more aggressive the cleaning operation is. However, most of the cleaning rates are decreasing with longer immersion times, which can be explained by the progressing removal of impurities from the surface. Thus the resistance against dissolution is increasing with cleaning time. However, this trend is not valid for all conditions thus other effects may play a role.

The differences in the time dependence of the cleaning rates between oxalic acid on the one hand and citric and acetic acid on the other hand may indicate that different mechanisms are involved. Although, within 30 s of immersion, the cleaning rate decreased slightly for all the three acids, it is only significantly reduced for oxalic acid while a gentle increase

was observed for acetic and citric acid with further increasing immersion time. This observed trend is attributed mainly to two different mechanisms. In the case of oxalic acid, there was a formation of surface film of metallic oxalate complexes, which significantly affected the cleaning rate. During immersion, this film rips off the surface due to poor adhesion leaving behind non protective brown spots of metallic oxalate complexes on the surface with more cleaning resistance. In the case of acetic and citric acids, there is material removal without formation of any surface film on the surface of the alloy. Here the formation of excessive hydrogen gas which was observed especially on the surfaces of specimens treated in the higher concentration acid solutions is an important factor influencing the cleaning rate. Such gas envelopes may prevent contact with the solution; and as a result, the cleaning rate may be reduced. It is observed that there is some incubation time before the excessive gas evolution starts reaching a maximum and finally decreasing again. The time for each period depends on the concentration of the acid and it correlates with the cleaning rate as a function of immersion time as shown in Fig. 2.

How efficient a cleaning treatment can be depends not only on the amount of material removed, but also on the reaction products of substrate and cleaning solution. The solubility product constants (K_{sp}) of the expected compounds which may form due to the reactions of the individual elements present in the alloy and each acid, are considered in Table 3. The higher the solubility product constant the more soluble the compound will be. If any of the salts formed is soluble, it means that it cannot form a protective film on the surface of the substrate. Therefore, the salts with a very low solubility product constant are considered insoluble and will form a layer on the surface of the substrate. From the information in Table 3, all the acetates formed are soluble in aqueous solution; therefore they cannot form a protective film on the surface of the substrate. This is evident from the micrographs presented in Fig. 7a and b. The oxalates of Mg, Al and Zn are insoluble in aqueous solution and their low solubility explains the observed layer formation during cleaning in oxalic acid. However, these oxalates formed on the surface of the substrate flake or rip off the surface leaving behind a brown spotted surface if the specimens are dried. The reason for this could be probably due to the poor adhesion of the oxalates on the substrate.

Consequently, there is no strong evidence of film formation on the micrograph for oxalic acid treated specimens as well (Fig. 7c and d). Thus the oxalic acid is suitable for cleaning AZ31, in spite of the non-soluble magnesium and aluminium oxalates forming. For the citrates, only Zn citrate is insoluble, citrates of Mg and Al are soluble. The formation of a protective film might not occur as a result of low amount of zinc as can be seen from the micrograph (Fig. 7e and f). There is also hydroxide film formation on the surfaces of the substrate after the cleaning process. This is due to the reaction with water during the rinsing process or water vapour or moisture in the atmosphere after the cleaning process. These hydroxides are insoluble in aqueous solution and can provide protective coverage to some extent on the surface of the substrate. However, from the hydroxide bands in the IR spectra (Fig. 8), the amount of hydroxides appears to be quite low and the hydroxide film may not be thick enough to be protective.

The compounds which can form by the impurity elements with the respective acids are given in Table 3 as well. It is obvious that the acetates of the impurity elements are all soluble in aqueous solution. This means these compounds will mostly go into the solution. Iron (III) oxalate is soluble in aqueous solution while the oxalates of the other impurity elements (copper and nickel) are insoluble. However, the soluble compound will dissolve in the solution while the insoluble oxalates will flake off the surface of the substrate together with the magnesium and aluminium oxalates, leaving the surface of the substrate free from the impurities. Nickel (II) citrates are soluble in aqueous solution and will subsequently dissolve into the solution while copper citrate is insoluble and might be redeposited on the surface of the substrate. According to literature the iron (III) citrate should be soluble as well (Table. 3). However our results indicate that the iron remain on the surface of citric acid cleaned specimens is on a much higher level compared with acetic or oxalic acid pickled specimens. This suggests that the iron is either present in a different oxidation state and/or the highly alkaline surface of Mg has a detrimental effect on the solubility. Summarising, one can state that the reduction in corrosion rate associated with cleaning in acetic, oxalic and citric acids is most likely a result of reducing the impurity level by material removal. The mechanism is mainly dissolution of the contaminated surface when

acetic or citric acid is used, while flaking off of non-soluble reaction products is mainly observed for oxalic acid. Thus most impurities form soluble organo-metallic complexes which dissolve together with the matrix leaving the metal surface free from impurities. The non-soluble impurities are simply falling to the bottom of the container if the surrounding matrix is removed. In both cases, redeposition should be prevented.

However, there is evidence that some conditions of treatment with oxalic and citric acids showed higher copper impurity level relative to the as-received specimen. Copper oxalate is sparingly soluble ($K_{sp} = 4.4 \times 10^{-10}$) and copper citrate and copper hydroxide are insoluble. So they are either not removed from the surface or they are redeposited on the substrate. This probably means that only acetic acid is suitable to remove copper. However, there is almost no copper impurity in the alloy which makes it more difficult to follow changes and enrichment in the concentration (Table 1).

To reduce the corrosion rate of Mg alloys all surface impurities should be removed or reduced through acid pickling. From the corrosion rates in salt spray test, it is clear that the corrosion resistance is enhanced with increasing material removal from the contaminated surface of the alloy which in turn depends on the concentration and immersion time of each acid pickling solution. This correlates very well with the measured remaining impurity level on the surfaces. Obviously re-deposition of previously dissolved impurities is not a major concern and the surfaces are getting cleaner with increasing cleaning times. The limit which is finally reached for acetic and oxalic acid is the impurity content of the bulk alloy itself. Only citric acid maintained higher iron contents after cleaning compared to the bulk iron content. Thus the best performance in SST was recorded for acetic acid with the highest material removal and lowest impurity level. This is followed by oxalic acid accordingly and finally citric acid. This is confirmed by the electrochemical studies as well.

The electrochemical impedance spectroscopy results revealed that all the specimens showed only one capacitive loop in the high frequency region and an inductive part in the lower frequency region. The high frequency capacitive loop is ascribed to charge transfer

resistance (R_p) at the substrate /electrolyte interface [13, 15, 17, 20] and/or an oxide film effect [14, 15, 17, 18, 20]. The inductive behaviour shows that the corrosion initiates as localized corrosion in the form of pits [21]. This is in agreement with the suggestion of Song and Atrens [4] that the predominant mechanism in magnesium alloys is localized pitting corrosion. It was observed that the specimens showed increased impedance with immersion time (Fig. 11). G. Galicia et al. [16] suggested that this could be due to accumulation of corrosion products at the electrode surface acting as a barrier. However cleaning effects involved with material removal by the corrosive solution, thereby reducing the amount of the impurities on the surfaces of the specimens further, may play an additional role. However, the presence of the inductive behaviour in all the specimens in the Nyquist plots shows that the surfaces still have some impurities or impurity containing intermetallics which caused the localized corrosion attack. It is probable that at longer immersion time like 20 hours, the corrosion process on the exposed surfaces of the specimens might have also removed some of these surface impurities thereby enhancing the corrosion resistance of these specimens. These impurities cause localized and galvanic corrosion on the matrix around them. This process removes the matrix preferentially to these impurities, causing undermining of the impurities which will fall to the bottom of the container. Furthermore, in the corrosion process there is also formation of $Mg(OH)_2$ protective film in agreement with G. Galicia et al.. However, longer immersion leads to partial breakdown of the protective layer due to the starting of localized corrosion attack [22]. The synergistic property of the cleaning effect of the corrosion process described above and the hydroxide film formation may be responsible for the improved resistance in chloride containing aqueous medium with increasing immersion times.

Nevertheless, the amount of material removed from the surface of the specimens during cleaning before electrochemical testing has the most significant influence on the corrosion resistance.

Finally, it should be pointed out that there are disadvantages in using oxalic and citric acids even though corrosion rates of less than 1 mm/year can be obtained for each acid in salt spray test. For citric acid the iron impurity level remained higher and therefore the corrosion rate is also remaining on a higher level compared to acetic and oxalic acid. The

disadvantage of oxalic acid is the formation of insoluble oxalates which form a film on the surface. This film can be quite easily removed from the surface because the adhesion is poor, but nevertheless it requires an additional handling step. Therefore, the first choice for an organic cleaning solution is still based on acetic acid. However, oxalic acid might be an alternative because similar impurity levels and corrosion rates can be obtained.

5. Conclusion

Organic acid cleaning processes have significantly reduced the surface impurity level of AZ31 Mg alloy sheet thereby reducing its corrosion susceptibility by reducing the formation of galvanic cells.

The reduction in corrosion rate in SST of specimens cleaned in acetic, oxalic and citric acids was mainly due to impurity removal, while two different mechanisms were identified. For acetic and citric acids, most of their salts are soluble in aqueous solution and cleaning of the surface is mainly by simultaneous dissolution of the matrix and impurities. No protective films form on the surfaces of the substrate. In contrast oxalates of Al and Mg and of most impurities are insoluble. They are forming deposits on the surface but due to poor adhesion, the layer is flaking off the substrate already during the pickling step. Consequently, this layer cannot render any protection to the surface. However, the advantage is that the impurities are removed also with the main magnesium and aluminium oxalate layer.

For all acids corrosion rates of less than 1 mm/year can be obtained by adjusting the concentration or immersion time. To obtain good corrosion resistance for AZ31 Mg alloy sheet, 4 μm etching seems to be sufficient requiring etching time less than or equal to 1 minute depending on the acid concentration. This will ensure a reduction in the impurity level reaching values around < 20 ppm for Fe and < 10 ppm for Ni on the surface of the alloy.

Summarising this study, it has been established that acetic acid based cleaning solutions are the better choice for cleaning AZ31 sheet compared to oxalic and citric acid solutions. Oxalic acid exhibits the disadvantage of the more difficult removal of the solid oxalate

reactions products from the surface, while citric acid revealed the poorest removal of iron impurities from the surface.

References

[1] J. E. Gray, B. Luan, Protective coatings on magnesium and its alloys - a critical review, Journal of Alloys and Compounds 336 (2002) 88 – 113.

[2] M. Ger, Y. Sung, W. Hwu, Y. Liu, Method for Treating Magnesium Alloy by Chemical Conversion, US 6755918 B 2 (2004).

[3] P. B. Srinivasan, C. Blawert, W. Dietzet, K. U. Kainer, Stress corrosion cracking behaviour of a surface-modified magnesium alloy, Scripta Materialia 59 (2008) 43 – 46.

[4] G. Song, A. Atrens, Understanding Magnesium Corrosion – a Framework for Improved Alloy Performance, Advanced Engineering Materials 12 (2003) 5, 837 – 858.

[5] A. Pardo, M. C. Merino, A. E. Coy, R. Arrabal, F. Viejo, E. Matykina, Corrrosion behaviour of Magnesium/aluminium alloys in 3.5 wt. % NaCl, Corrosion Science 50 (2008) 823 – 834.

[6] G. Song, A. Atrens, Recent insights into the mechanism of magnesium corrosion and research suggestions, Advanced Engineering Materials 9 (2003) 3, 177 – 183.

[7] N. Shikata, Y. Kondou, Y. Nishikawa, Y. Nishizawa, Y. Sakamoto, T. Fujiwaki, Surface- Treated Article of Magnesium or Magnesium Alloys: Method of Surface-Preparation and Method of Coating Patent Cooperation Treaty (PCT), (1999).

[8] Metals Handbook, Volume 5, 9th Ed; Surface Cleaning, Finishing and Coating, ASM International, USA, 1994.

[9] G. Yan, W.Guixiang, D.Guojun, G. Fan, Z. Lili, Z. Milin, Corrosion resistance of anodized AZ31 Mg alloy in borate solution containing titania sol, Journal of Alloys and Compounds 478 (2008) 458 – 461.

[10] R. Supplit, T. Koch, U. Schubert, Evaluation of the anti-corrosive effect of acid pickling and sol-gel coating on magnesium AZ31 alloy, Corrosion Science 49 (2007) 3015 – 3023.

[11] U. C. Nwaogu, C. Blawert, N. Scharnagl, W. Dietzel, K. U. Kainer, Influence of inorganic acid pickling on the corrosion resistance of magnesium alloy AZ31 sheet, Corrosion Science 51 (2009) 2544 – 2556.

[12] S. Aleksovska, V. M. Petruševski, B. Šoptrajanov, Infrared spectra of the monohydrates of manganes (III) phosphate and manganese (III) arsenate: relation to

the compounds of the Kieserite family, Journal of Molecular Structure 408/409 (1997) 413 – 416.

[13] G. B. Hamu, D. Eliezer, L. Wagner, The relationship between severe plastic deformation microstructure and corrosion behaviour of AZ31 magnesium alloys, Journal of Alloy and Compounds 468 (2009) 222 – 229.

[14] H. Ardelean, I. Frateur, S. Zanna, A. Atrens, P. Marcus,Corrosion peotection of AZ91 magnesium alloy by anodizing in niobium and zirconium-containing electrolytes, Corrosion Science 51 (2009) 3030 – 3038.

[15] R. Rosliza, W. B. Wan Nik, S. Izman, Y. Prawoto, Anti-corrosive properties of natural honey on Al-Mg-Si alloy in sea water, Current Applied Physics, xxx (2009) xxx – xxx.

[16] G. Galicia, N. Pébére, B. Tribollet, V. Vivier, Local and global electrochemical Impedances applied to the corrosion behaviour of AZ91 magnesium alloy, Corrosion Science 51 (2009) 1789 – 1794.

[17] M. Anik, G. Celikten, Analysis of the electrochemical reaction behaviour of alloy by EIS technique in H_3PO_4/KOH buffered K_2SO_4 solutions, Corrosion Science (2007) 1878 – 1894.

[18] K. Y. Chiu, M. H. Wong, F. T. Cheng, H. C. Man, Characterization and corrosion studies of fluoride conversion coating on degradable Mg implants, Surface and Coating Technology 202 (2007) 590 – 598.

[19] W. Liu, F. Cao, A. Chen, L. Chang, J. Zhang, C. Cao, Corrosion behaviour of AM60 Magnesium alloys containing Ce or La under thin electrolyte layers. Part 1: Microstructural characterization and electrochemical behaviour, Corrosion Science 52 (2010) 627 – 638.

[20] H. Ardelean, I. Frateur, P. Marcus, Corrosion protection of magnesium alloys by cerium, zirconium and niobium-based conversion coatings, Corrosion Science 50 (2008) 1907 – 1918.

[21]. R. Ghosh, D. D. N. Singh, Kinetics, mechanism and characterization of passive film formed on hot dip galvanized coating exposed in simulated concrete pore solution, Surface and Coatings Technology 201 (2007) 7346 – 7359.

[22] S. V. Lamaka, M. F. Montemor, A. F. Galio, M. L. Zheludkeich, C. Trindade, L. F. Dick, M. G. S. Ferreira, Novel hybrid sol-gel coatings for corrosion protection of AZ 31B magnesium alloy, Electrochemica Acta 53 (2008) 4773 – 4783.

[23] David R. Lide, H. P. R. Frederike (Eds.), Solubility and Solubility Product of Compounds, 78th Edition, CRC Handbook of Chemistry and Physics, New York, 1996, 8 - 106.

Figure Captions

Fig. 1: Variation of material removed with immersion time for different concentrations of (a) acetic, (b) oxalic and (c) citric acids.

Fig. 2: Variation of cleaning rates with immersion time for different concentrations of (a) acetic, (b) oxalic and (c) citric acids

Fig. 3: Variation of surface roughness with material removed for each of the concentrations of acetic, oxalic and citric acids at all the immersion times.

Fig. 4: Variation of impurity levels with material removed for all the treatments in the three different concentrations of acetic, oxalic and citric acids as determined by Spark-discharge optical emission spectroscopy.

Fig. 5: Variation of corrosion rates in salt spray test with material removed for all the treatments in the three different concentrations of acetic, oxalic and citric acids at different immersion times.

Fig. 6: SEM micrograph of the surface of as-received specimen.

Fig. 7: SEM micrographs of selected treatments for each of the acids (a and b for acetic acid, c and d for oxalic acid and e and f for citric acid; a, c, and e, best conditions and b, d and f, worst conditions in salt spray test).

Fig. 8: IR spectra of surfaces of (a) as-received specimen and specimens cleaned in (b) acetic, (c) oxalic and (d) citric acids with the best corrosion behaviour in salt spray test.

Fig. 9: Micrographs illustrating locations of points for EDX spot analysis of (a) as-received specimen and selected treatments with best conditions for (b) acetic, (c) oxalic and (d) citric acids.

Fig. 10: Impurity levels on the surfaces of as-received (AR surface); bulk and selected treated specimens with (a) best and (b) worst corrosion behaviour in salt spray test for acetic (AA), oxalic (OA) and citric (CA) acids by spark discharge-optical emission spectroscopy.

Fig. 11: Nyquist plots (EIS) of as-received and treated specimens cleaned in various acids with the best corrosion behaviour in salt spray test after (a) 2 and (b) 20 hours of exposure to neutral 5 % NaCl solution.

Table 1: Chemical composition (in wt %) of AZ31 magnesium alloy.

Description		Al	Zn	Mn	Si	Cu	Ca	Ni	Fe	Mg
As-received	Surface	2.970	0.845	0.236	0.0226	0.002	0.003	0.004	0.026	Bal.
	Bulk	2.870	0.812	0.248	0.0224	0.001	0.005	0.001	0.002	Bal.
Standard		3.000	1.000	<0.500	<0.100	<0.005	-	<0.002	<0.005	Bal.

Table 2: Bath composition and operating conditions of cleaning AZ 31 Mg alloy sheet.

Process	Operation	Composition of cleaning bath	Conc. (g/l)	pH	Time (s) of immersion in each bath concentration
1	Alkaline cleaning	Sodium hydroxide, NaOH	40	13.6	60
2	Acid cleaning	Acetic acid, CH_3COOH and Calcium nitrate, $Ca(NO_3)_2$	100 (50)[a]	2.23	15, 30, 60, 120
			200 (50)[a]	2.00	
			300 (50)[a]	1.84	
		Oxalic acid, $C_2H_2O_4.2H_2O$	20	1.58	
			40	1.44	
			80	1.29	
		Citric acid, $C_6H_8O_7$	40	2.27	
			80	2.09	
			120	2.00	

Note (a) The numbers inside brackets under conc. represent the concentration of $Ca(NO_3)_2$

Table 3: Alloying and impurity elements' phases formed during immersion in each acid and solubility conditions in aqueous solutions [23].

	All acids	K_{sp}	AA	K_{sp}	OA	K_{sp}	CA	K_{sp}
Mg	$Mg(OH)_2$	$5.6x10^{-12}$	$Mg(CH_3COO)_2$	soluble	MgC_2O_4	$4.8x10^{-6}$	$Mg_3(C_6H_5O_7)_2$	soluble
Al	$Al(OH)_3$	$3.0x10^{-3}$	$Al(CH_3COO)_3$	soluble	$Al_2(C_2O_4)_3$	insoluble	$AlC_6H_5O_7$	soluble
Zn	$Zn(OH)_2$	$3.0x10^{-17}$	$Zn(CH_3COO)_2$	soluble	ZnC_2O_4	$1.4x10^{-9}$	$Zn_3(C_6H_5O_7)_2$	insoluble
Fe	$Fe(OH)_2$	$2.6x10^{-39}$	$Fe(CH_3COO)_3$	soluble	$Fe_2(C_2O_4)_3$	soluble	$FeC_6H_5O_7$	soluble
Cu	$Cu(OH)_2$	insoluble	$Cu(CH_3COO)_2$	soluble	CuC_2O_4	4.4×10^{-10}	$Cu_3(C_6H_5O_7)_2$	insoluble
Ni	$Ni(OH)_2$	$5.5x10^{-16}$	$Ni(CH_3COO)_2$	soluble	NiC_2O_4	insoluble	$Ni_3(C_6H_5O_7)_2$	soluble

AA = Acetic acid, OA = Oxalic acid and CA = Citric acid

Table 4: Best conditions for each acid in SST

Acid	Conc. (g/l)	Immersion Time (s)	Mat. removed (μm)	Corr. rate (mm/yr)	Impurity Level (ppm)		
					Cu	Fe	Ni
Acetic acid	300	120	21.23 ± 1.52	0.34 ± 0.04	12.5	18.3	8.4
Oxalic acid	80	30	8.41 ± 1.01	0.59 ± 0.11	14.4	21.4	8.2
Citric acid	80	60	4.33 ± 0.28	0.72 ± 0.07	14.2	79.2	10.4

Table 5: Worst conditions for each acid in SST

Acid	Conc. (g/l)	Immersion Time (s)	Mat. removed (μm)	Corr. rate (mm/yr)	Impurity Level (ppm)		
					Cu	Fe	Ni
Acetic acid	200	15	2.09 ± 0.18	5.38 ± 0.80	13.3	37.1	10.8
Oxalic acid	20	15	0.58 ± 0.06	9.48 ± 0.22	16.9	161.0	15.0
Citric acid	40	15	0.65 ± 0.08	5.96 ± 0.81	16.2	160.0	22.2

Table 6: % elemental composition of the points analyzed with EDX for as-received (AR), acetic (AA), oxalic (CA) and citric (CA) acid treated specimens with the best corrosion behaviour in SST.

	Points	Weight % composition															
		C	O	Na	Cu	Mg	Al	Zn	Mn	Si	P	S	Cl	K	Ca	Cr	Fe
AR	P1	-	0.86	-	1.69	93.30	3.33	0.83	-	-	-	-	-	-	-	-	-
	P2	60.79	11.70	-	-	18.11	1.50	-	-	0.30	0.09	0.79	2.35	0.76	0.87	0.43	2.30
	P3	-	7.66	-	-	5.03	0.08	-	-	0.43	-	-	-	-	-	1.07	85.74
	Matrix	-	6.81	-	1.49	87.37	2.52	0.70	-	0.31	-	-	-	-	-	-	0.80
AA	P1	-	17.37	-	-	26.68	11.38	37.03	7.53	-	-	-	-	-	-	-	-
	P2	-	11.97	-	-	11.65	33.35	20.80	22.23	-	-	-	-	-	-	0.28	-
	P3	-	15.41	-	-	30.68	1.24	42.57	0.16	9.67	-	-	-	-	-	0.35	0.28
	Matrix	-	2.38	-	-	92.39	3.56	1.33	0.22	0.12	-	-	-	-	-	-	-
OA	P1	-	15.22	-	-	65.13	4.10	13.48	1.59	0.48	-	-	-	-	-	-	-
	P2	-	3.88	-	-	91.23	2.95	1.74	0.20	-	-	-	-	-	-	-	-
	P3		4.64	-	-	15.28	48.39	1.73	30.07	-	-	-	-	-	-	-	-
	P4	-	2.34	-	-	64.13	0.11	0.38	0.32	30.48	-	-	-	-	-	-	-
	Matrix	-	3.35	-	-	91.03	3.38	1.83	0.24	0.17	-	-	-	-	-	-	-
CA	P1	-	3.21	1.82	-	89.59	2.35	2.91	-	0.10	-	-	-	-	-	-	-
	P2	1.85	3.64	1.62	-	21.08	30.51	2.27	37.71	1.13	-	-	-	-	-	-	-
	P3	1.49	3.05	2.07	-	88.76	1.88	2.47	0.19	0.10	-	-	-	-	-	-	-
	P4	1.97	35.05	1.06	-	58.99	0.83	0.55	0.13	1.44	-	-	-	-	-	-	-
	P5	2.06	3.79	1.11	-	2.52	55.30	1.63	31.98	0.08	0.32	-	-	-	-	-	1.21
	Matrix	-	4.61	2.58	-	85.92	2.81	3.16	0.41	0.17	0.23	-	-	-	-	-	0.11

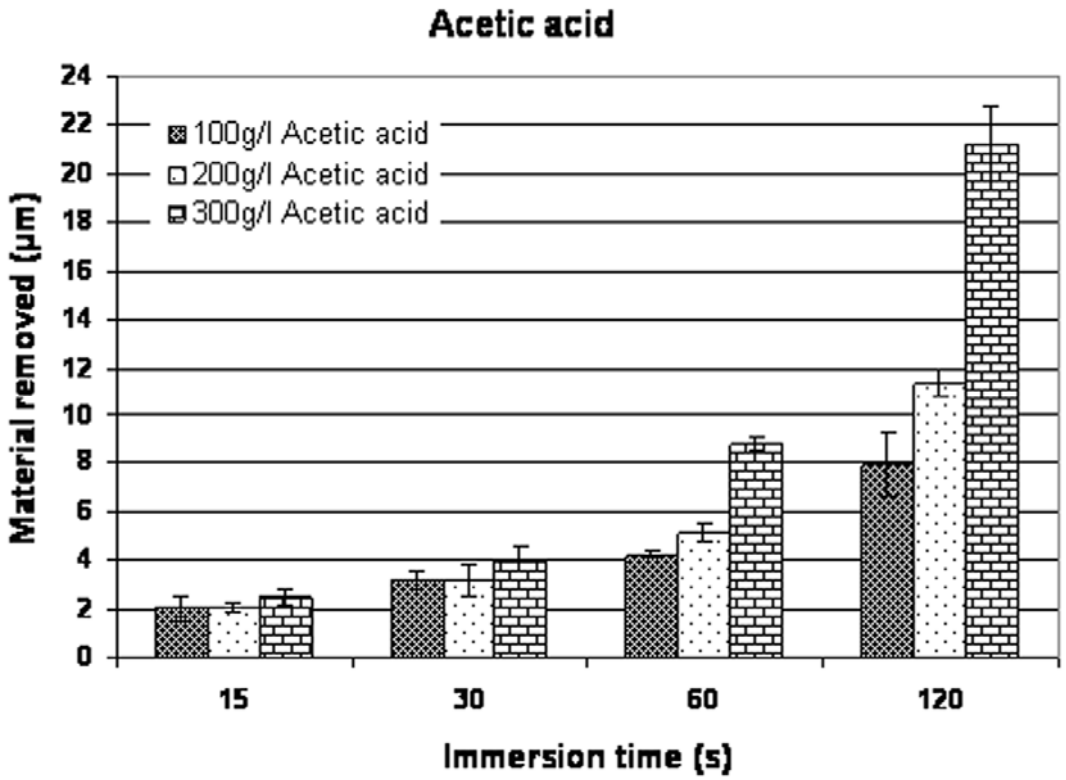
Acetic acid
100g/l Acetic acid
200g/l Acetic acid
300g/l Acetic acid
Material removed (µm)
24
22
20
18
16
14
12
10
8
6
4
2
0
15
30
60
120
Immersion time (s)

Fig. 1a

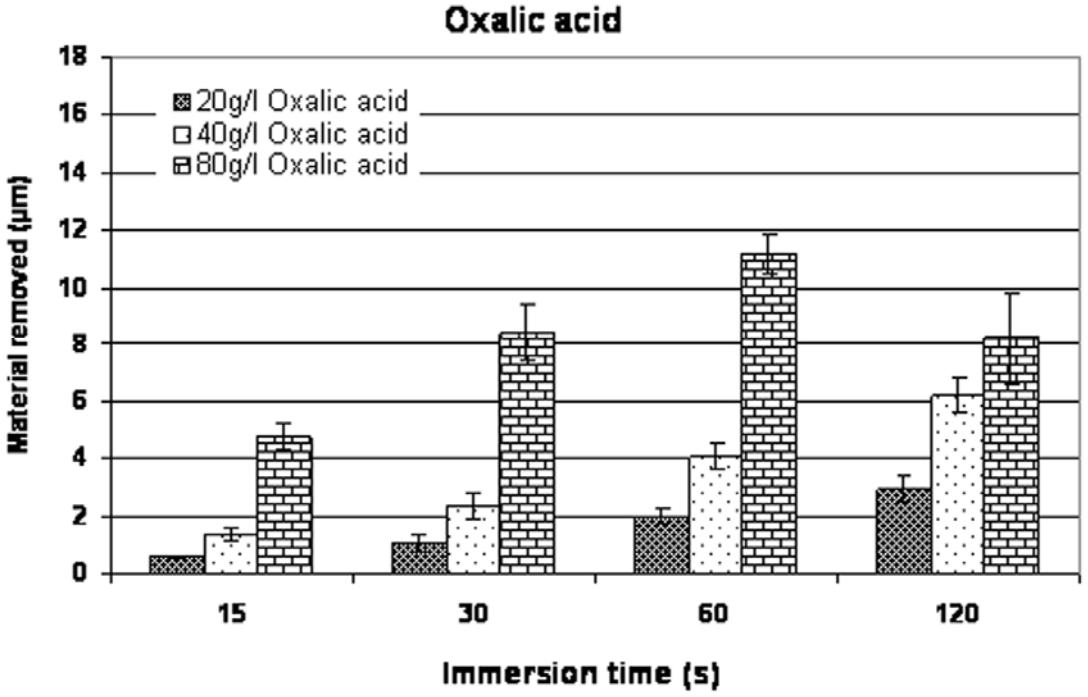
Oxalic acid
20g/l Oxalic acid
40g/l Oxalic acid
80g/l Oxalic acid
Material removed (µm)
0
2
4
6
8
10
12
14
16
18
15
30
60
120
Immersion time (s)

Fig. 1b

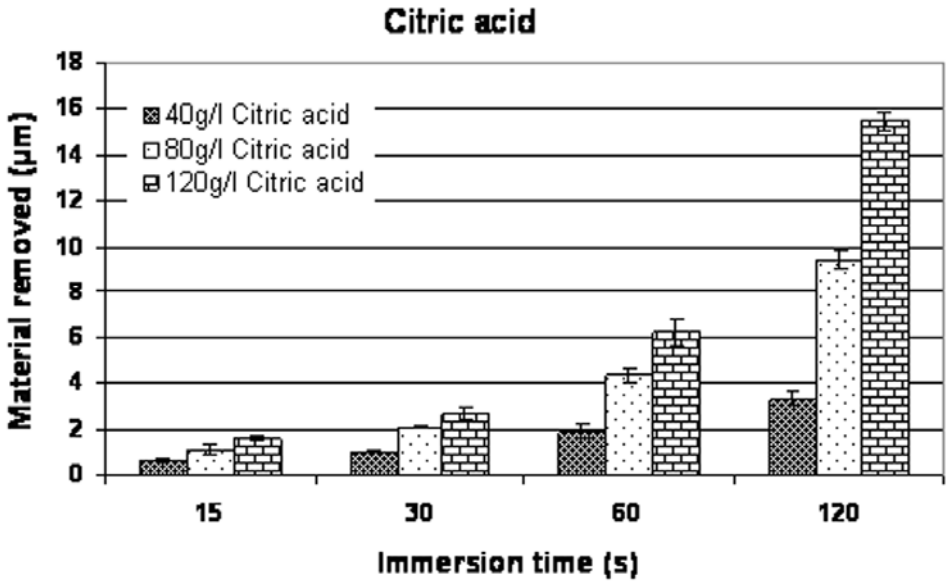
Citric acid
Material removed (µm)
18
16
14
12
10
8
6
4
2
0
40g/l Citric acid
80g/l Citric acid
120g/l Citric acid
15
30
60
120
Immersion time (s)

Fig. 1c

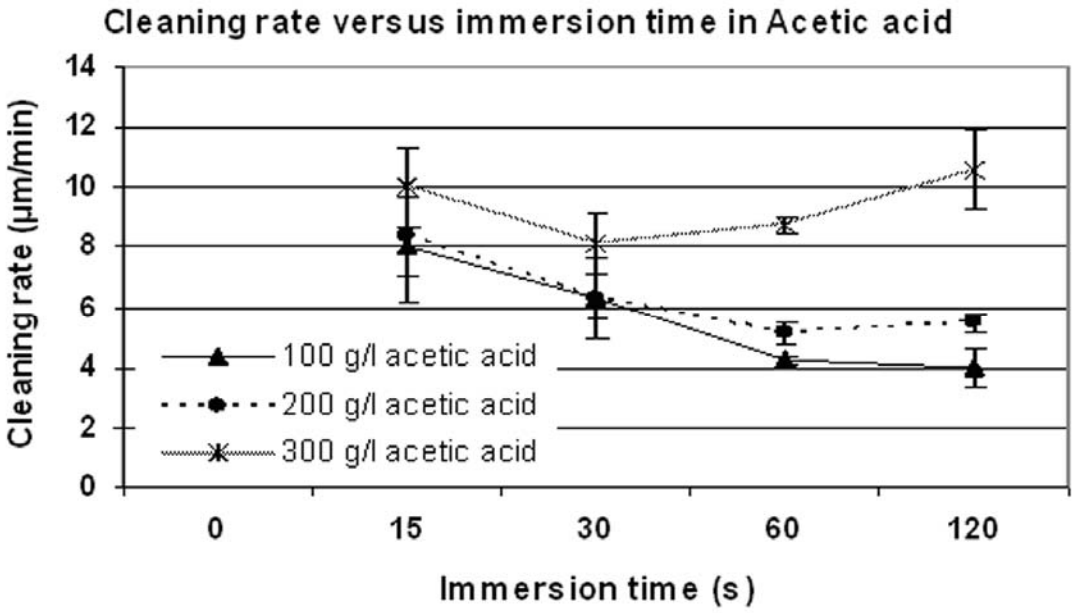
Cleaning rate versus immersion time in Acetic acid
Cleaning rate (µm/min)
14
12
10
8
6
4
2
0
100 g/l acetic acid
200 g/l acetic acid
300 g/l acetic acid
0
15
30
60
120
Immersion time (s)

Fig. 2a

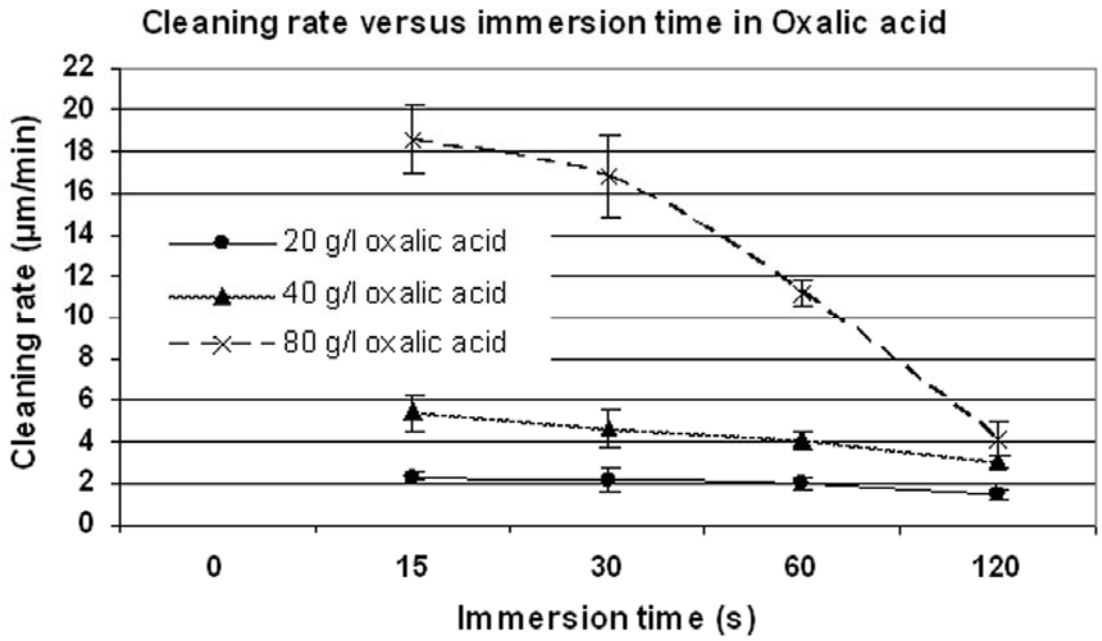
Cleaning rate versus immersion time in Oxalic acid
Cleaning rate (µm/min)
22
20
18
16
14
12
10
8
6
4
2
0
20 g/l oxalic acid
40 g/l oxalic acid
80 g/l oxalic acid
0
15
30
60
120
Immersion time (s)

Fig. 2b

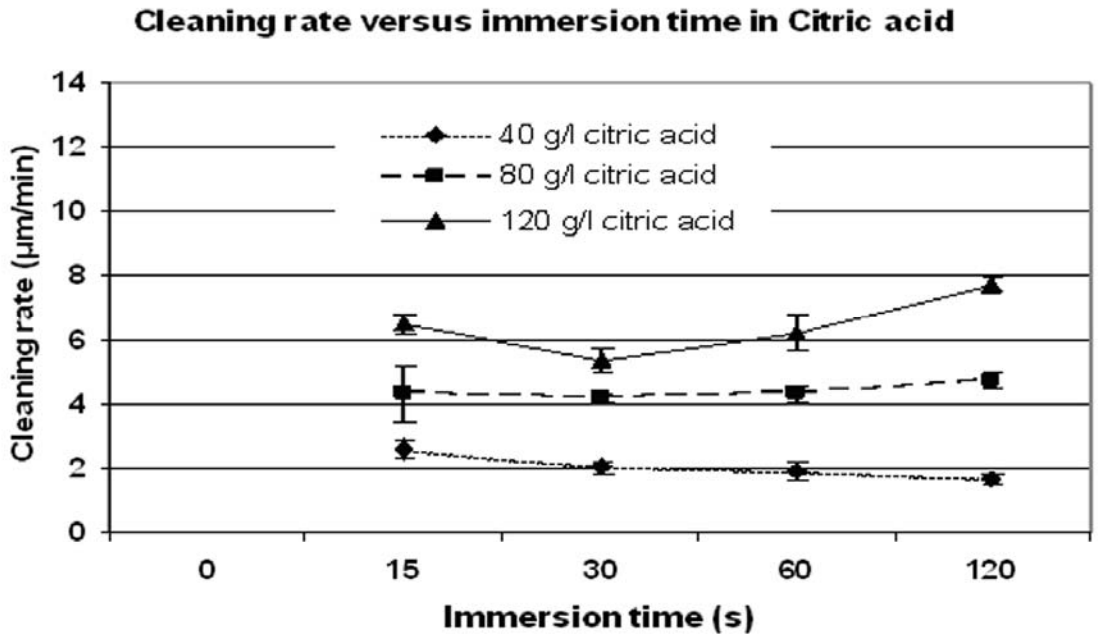
Cleaning rate versus immersion time in Citric acid
Cleaning rate (µm/min)
14
12
10
8
6
4
2
0
40 g/l citric acid
80 g/l citric acid
120 g/l citric acid
0
15
30
60
120
Immersion time (s)

Fig. 2c

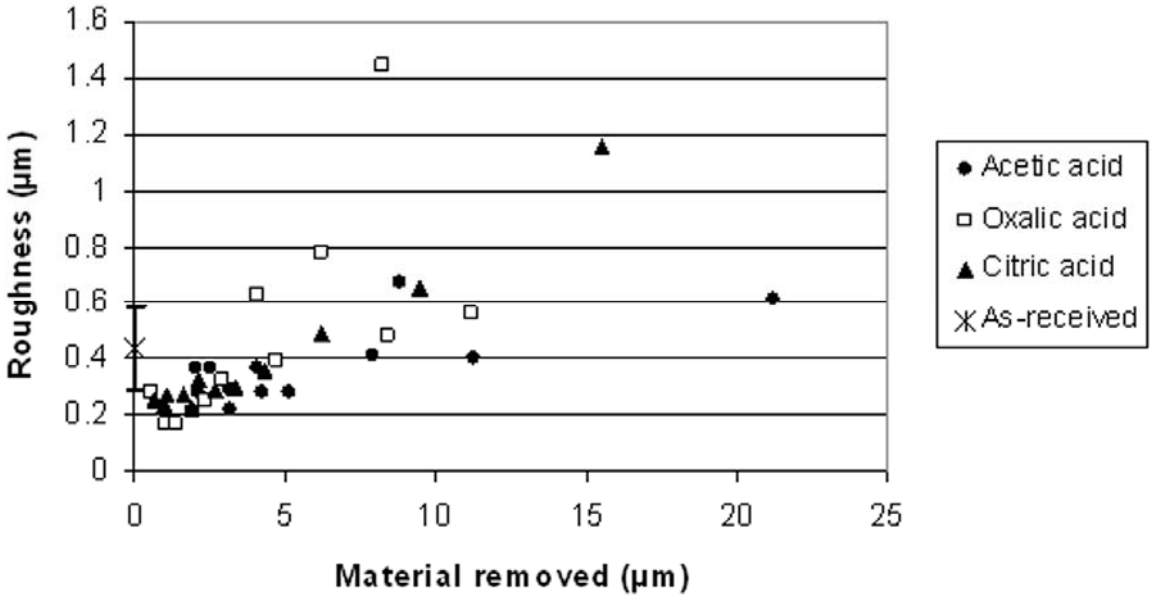
Roughness (µm)
1.6
1.4
1.2
1
0.8
0.6
0.4
0.2
0
0
5
10
15
20
25
Material removed (µm)
Acetic acid
Oxalic acid
Citric acid
As-received

Fig. 3

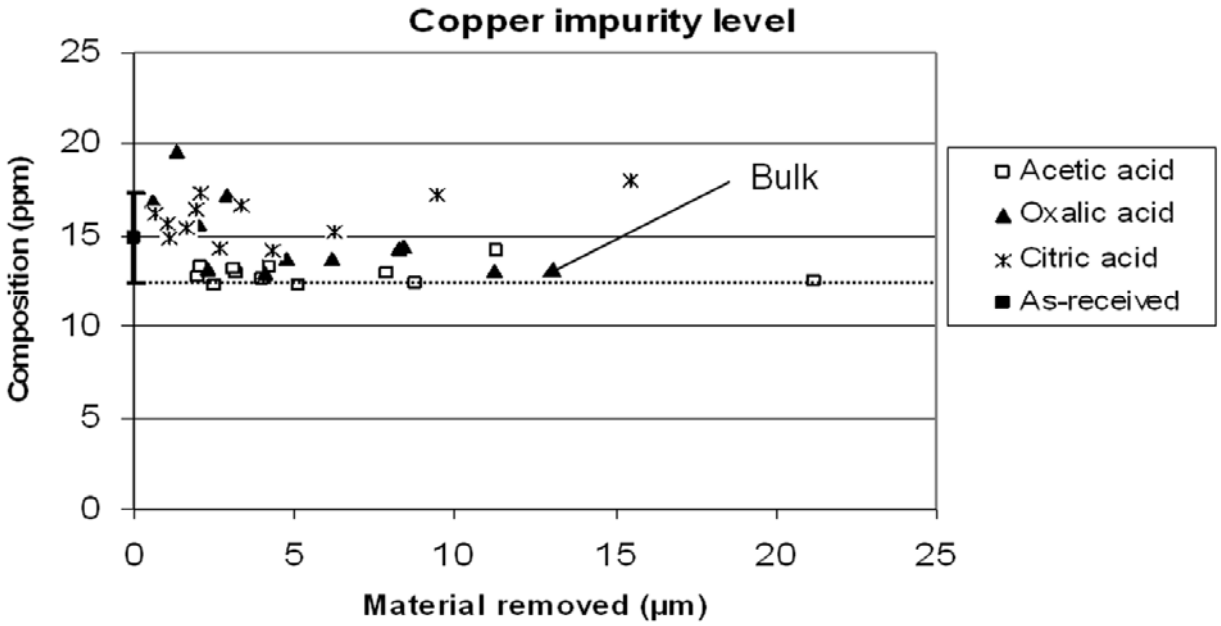
Copper impurity level
Composition (ppm)
25
20
15
10
5
0
0
5
10
15
20
25
Material removed (µm)
Bulk
Acetic acid
Oxalic acid
Citric acid
As-received

Fig. 4a

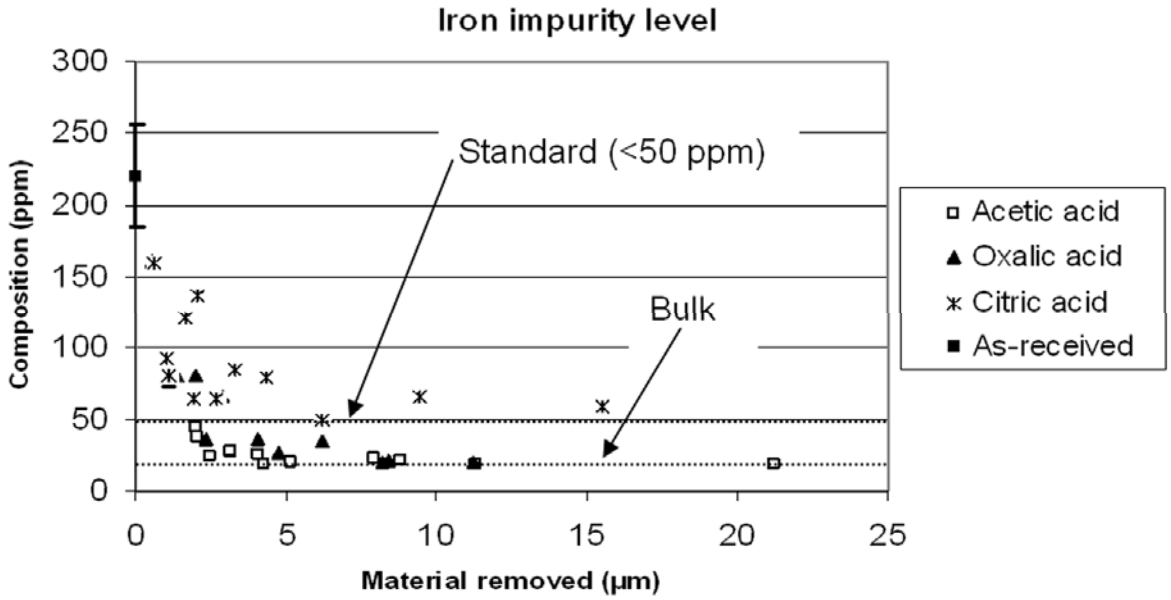
Iron impurity level
300
250
200
150
100
50
0
Composition (ppm)
Standard (<50 ppm)
Bulk
0
5
10
15
20
25
Material removed (µm)
Acetic acid
Oxalic acid
Citric acid
As-received

Fig. 4b

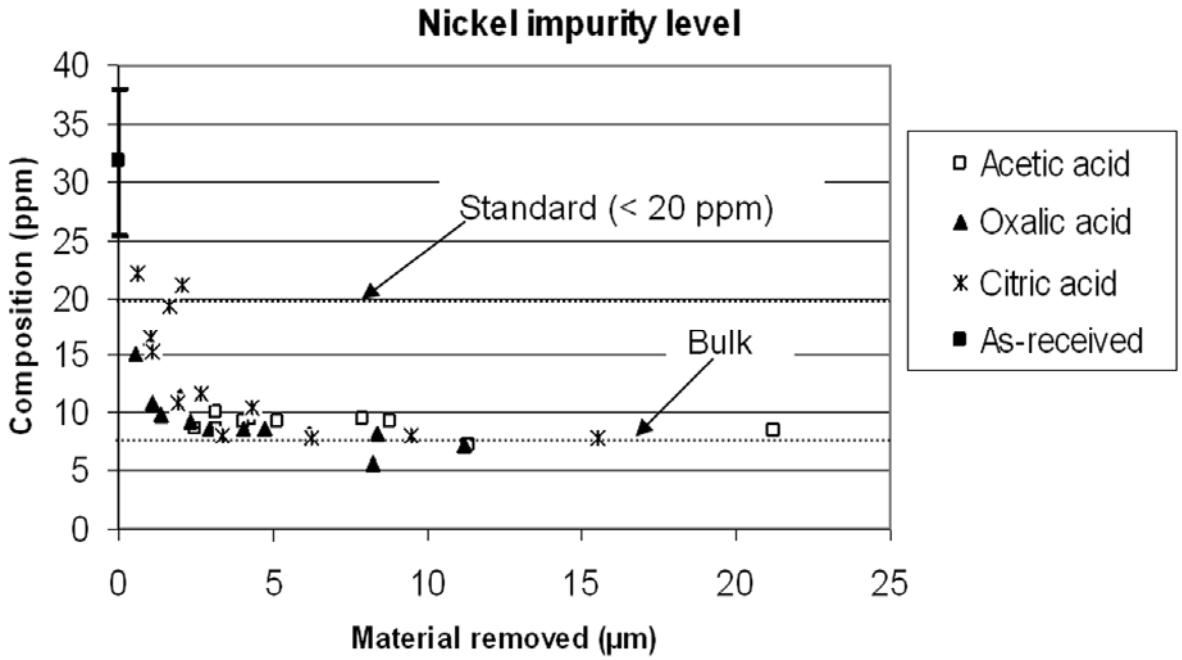
Nickel impurity level
Composition (ppm)
Material removed (µm)
Standard (< 20 ppm)
Bulk
Acetic acid
Oxalic acid
Citric acid
As-received
0
5
10
15
20
25
30
35
40

Fig. 4c

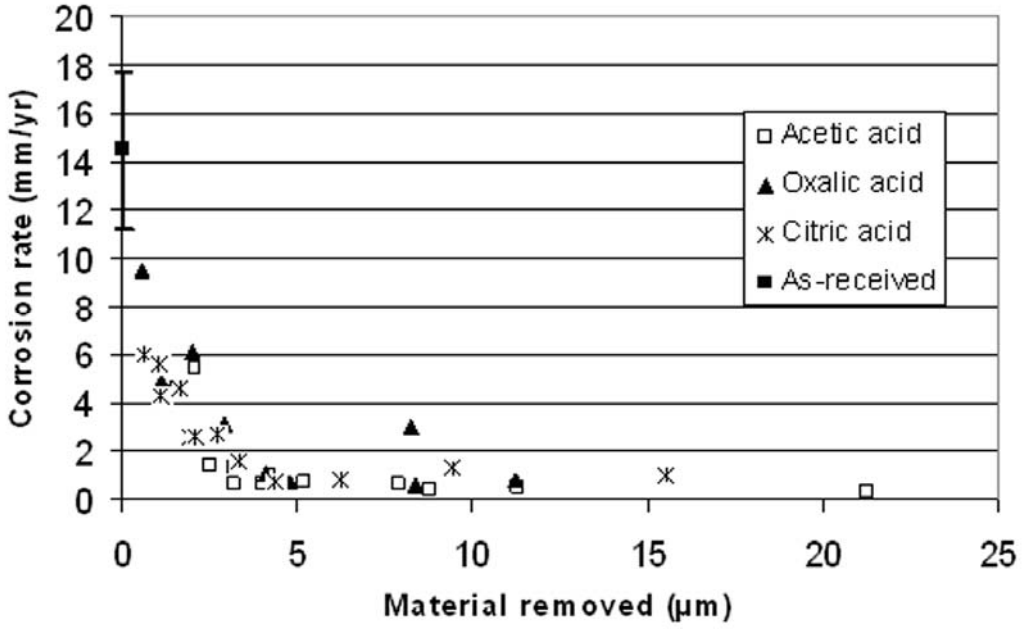
Corrosion rate (mm/yr)
Material removed (µm)
Acetic acid
Oxalic acid
Citric acid
As-received
0
2
4
6
8
10
12
14
16
18
20
0
5
10
15
20
25

Fig. 5

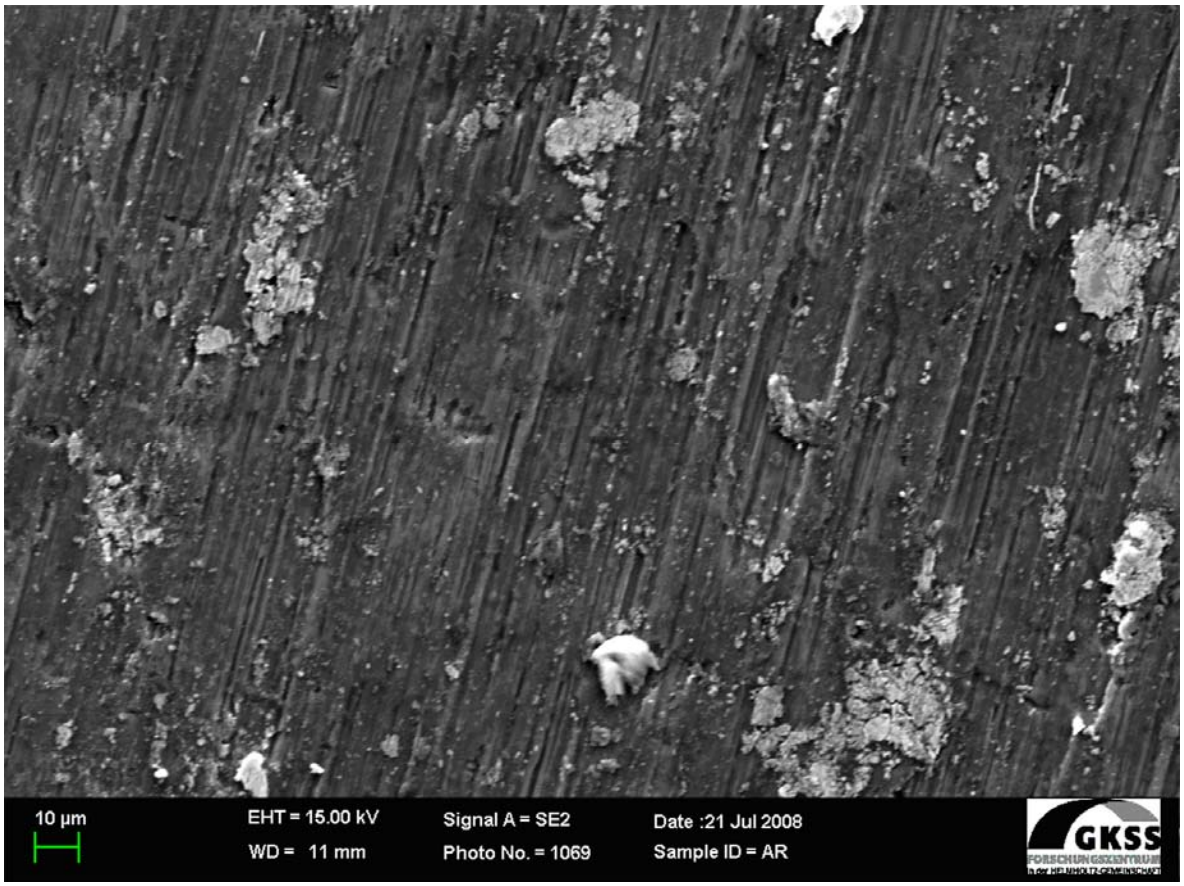
10 µm
EHT = 15.00 kV
WD = 11 mm
Signal A = SE2
Photo No. = 1069
Date :21 Jul 2008
Sample ID = AR
GKSS

Fig. 6

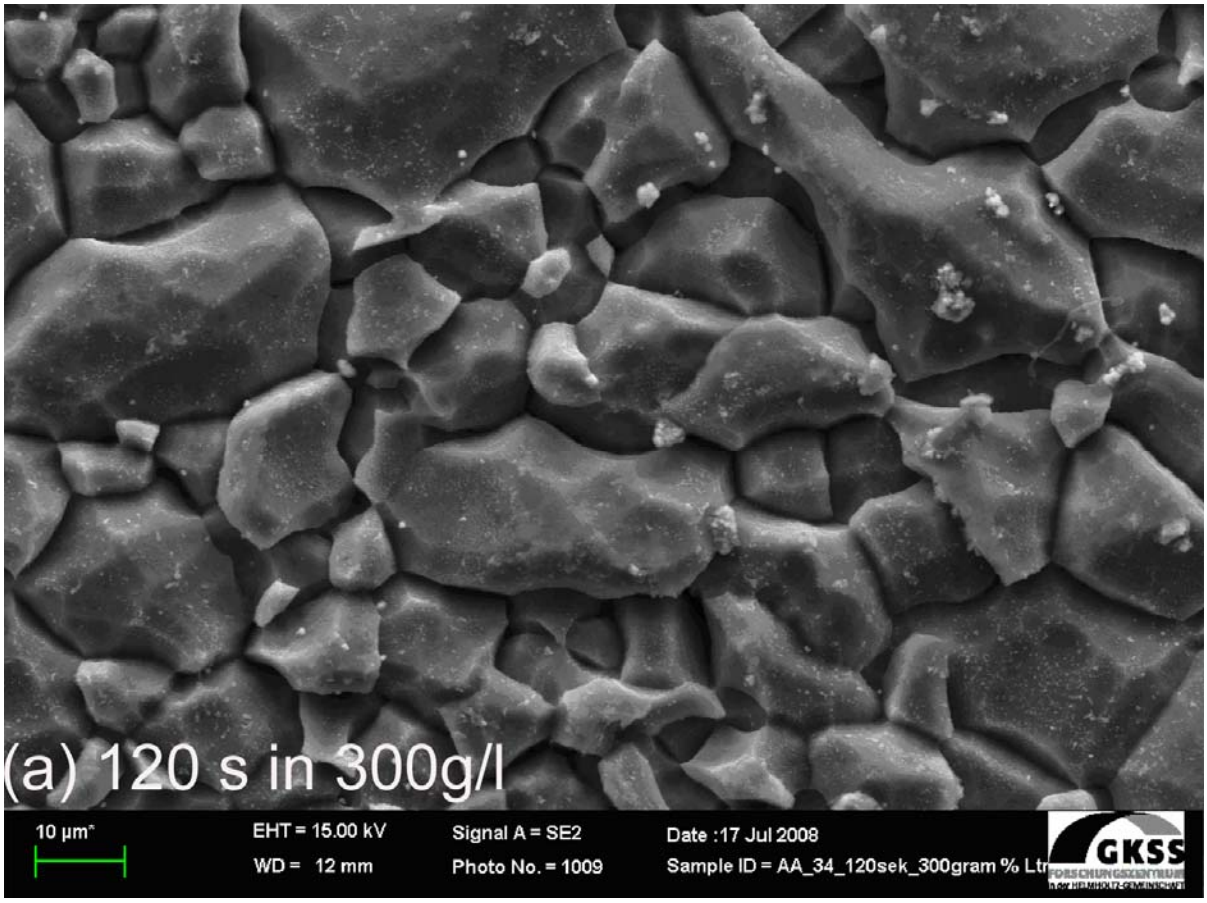
(a) 120 s in 300g/l
10 µm
EHT = 15.00 kV
WD = 12 mm
Signal A = SE2
Photo No. = 1009
Date :17 Jul 2008
Sample ID = AA_34_120sek_300gram % Ltr
GKSS

Fig. 7a

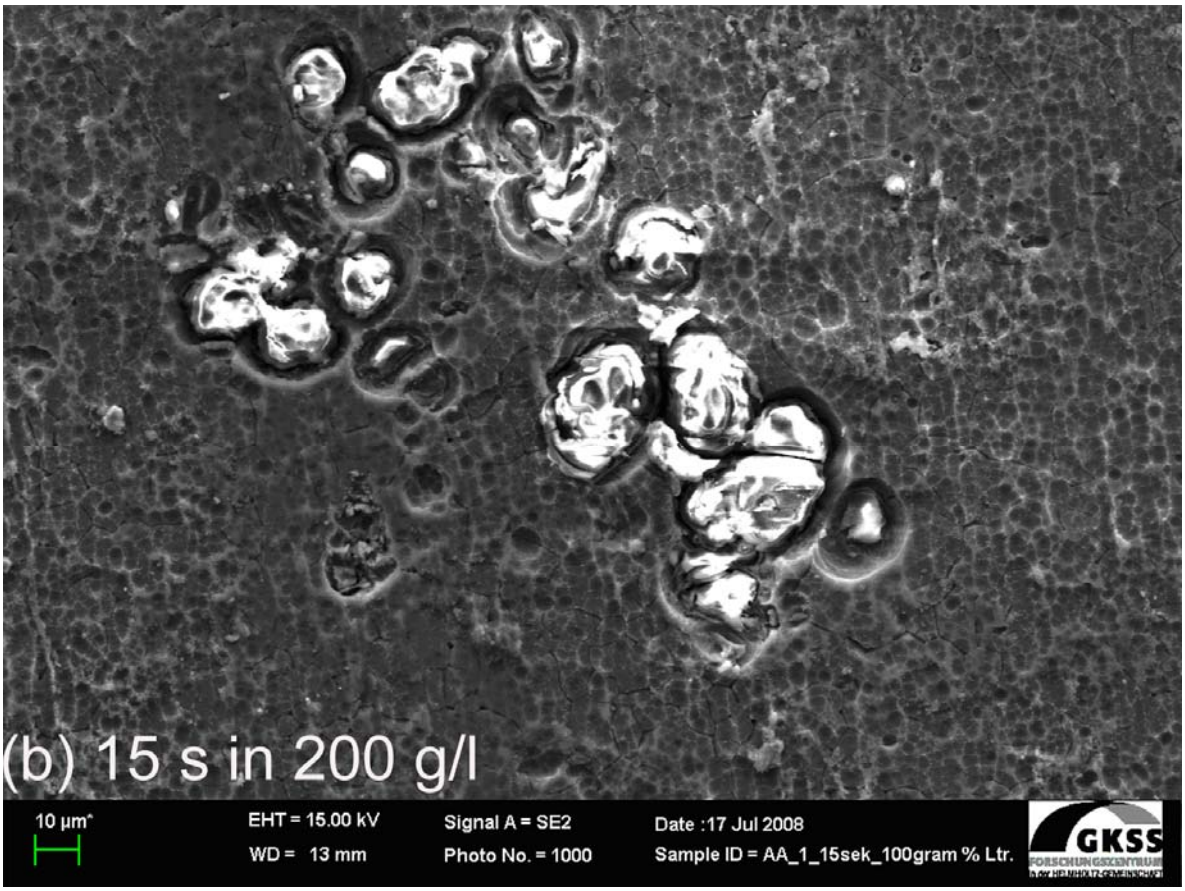
(b) 15 s in 200 g/l
10 µm*
EHT = 15.00 kV
WD = 13 mm
Signal A = SE2
Photo No. = 1000
Date :17 Jul 2008
Sample ID = AA_1_15sek_100gram % Ltr.
GKSS

Fig. 7b

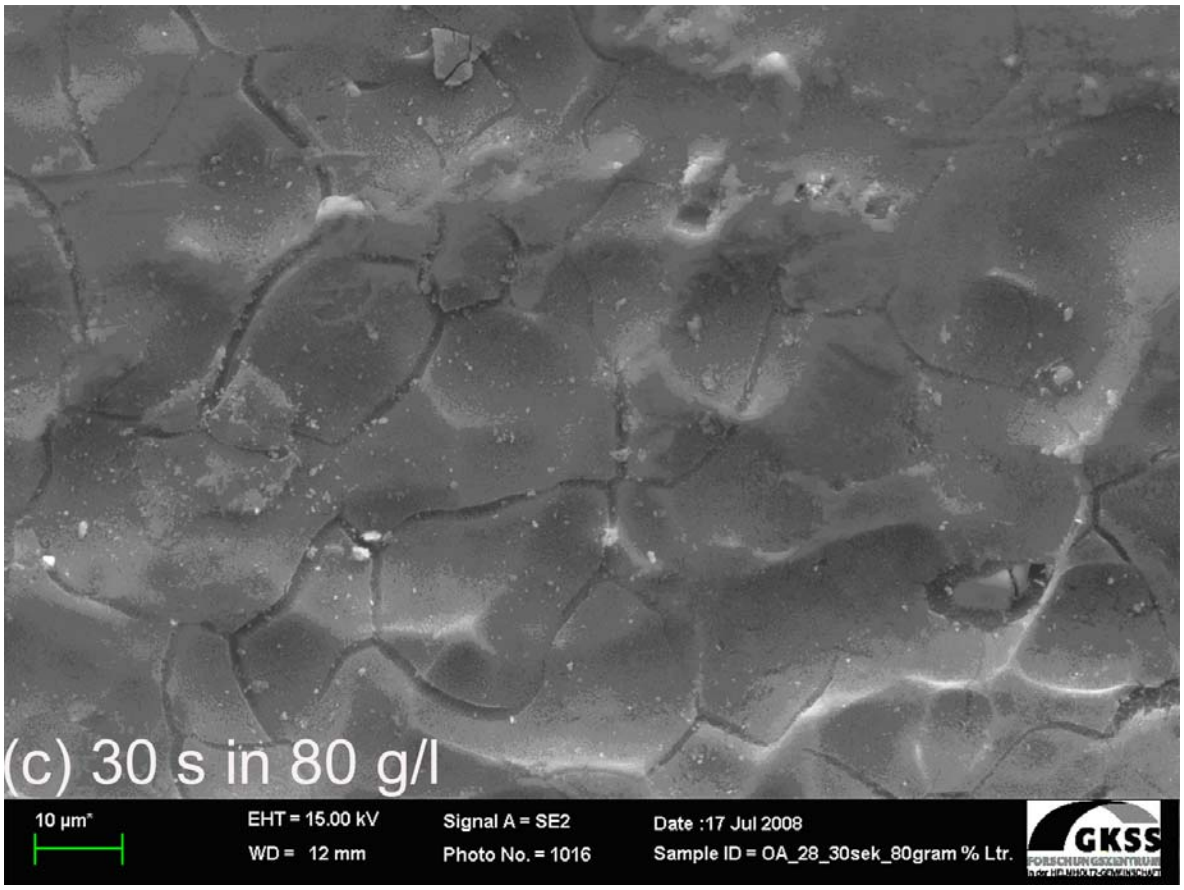
(c) 30 s in 80 g/l
10 µm
EHT = 15.00 kV
WD = 12 mm
Signal A = SE2
Photo No. = 1016
Date :17 Jul 2008
Sample ID = OA_28_30sek_80gram % Ltr.
GKSS

Fig. 7c

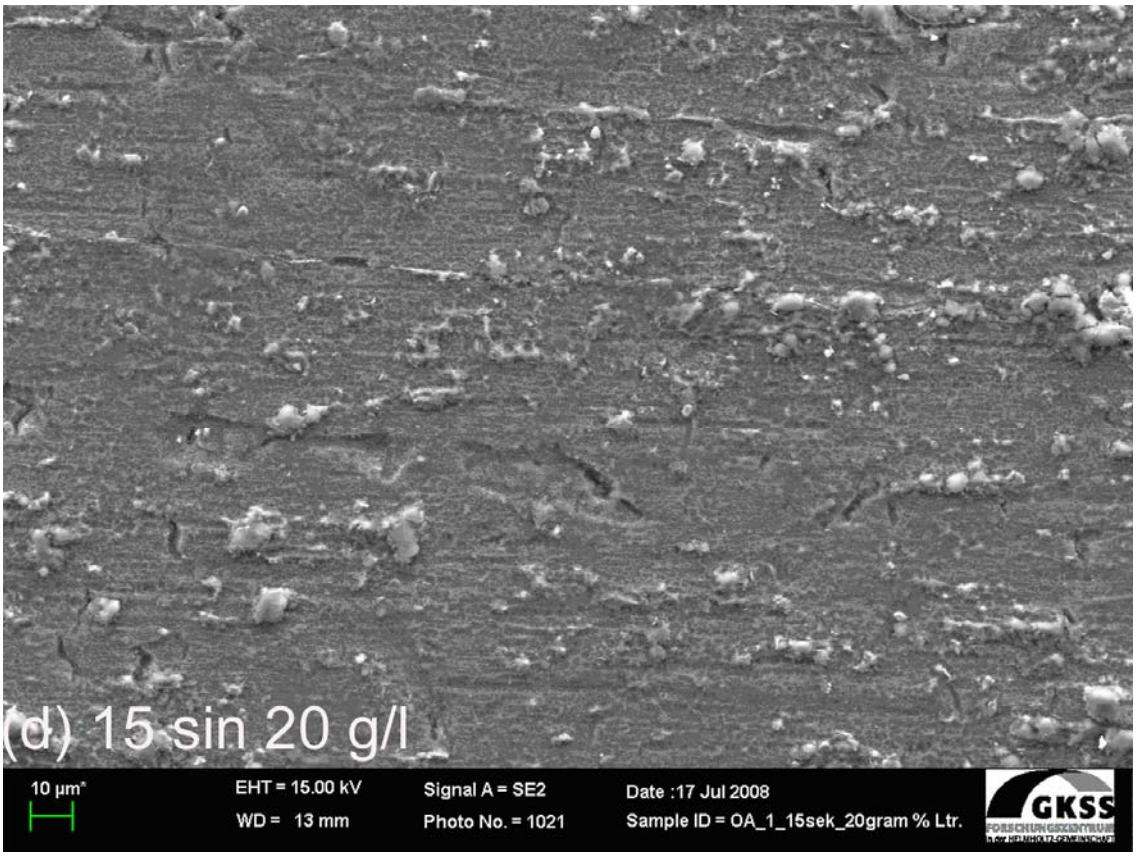
(d) 15 sin 20 g/l
10 µm
EHT = 15.00 kV
WD = 13 mm
Signal A = SE2
Photo No. = 1021
Date :17 Jul 2008
Sample ID = OA_1_15sek_20gram % Ltr.
GKSS

Fig. 7d

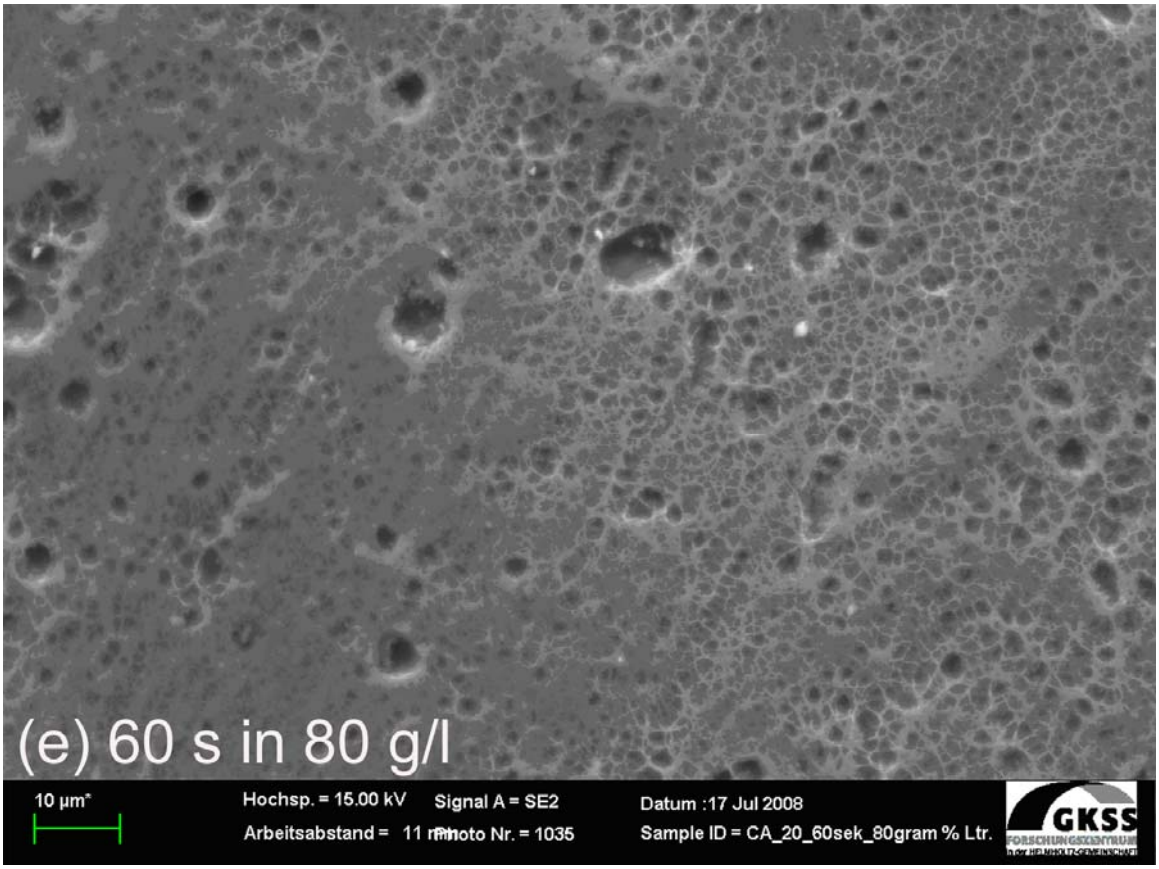
(e) 60 s in 80 g/l
10 µm*
Hochsp. = 15.00 kV
Signal A = SE2
Arbeitsabstand = 11 mm
Photo Nr. = 1035
Datum :17 Jul 2008
Sample ID = CA_20_60sek_80gram % Ltr.
GKSS

Fig. 7e

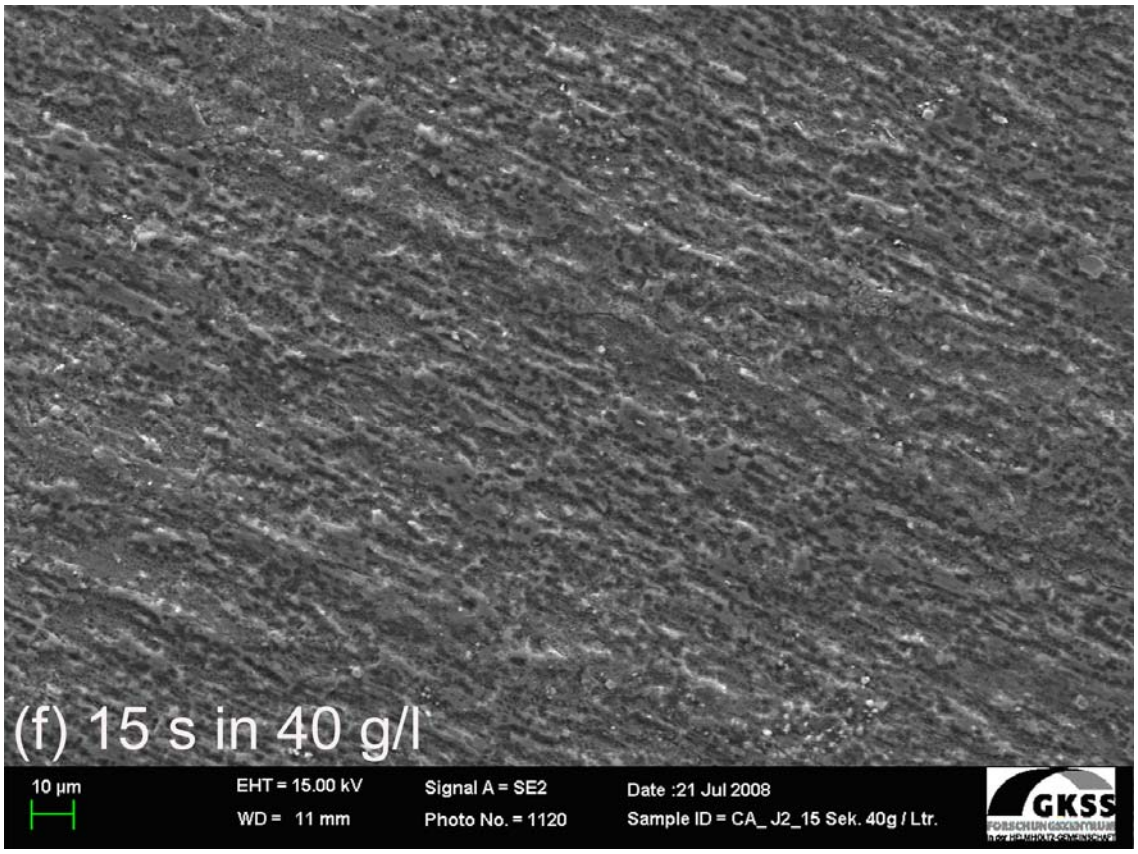
(f) 15 s in 40 g/l
10 µm
EHT = 15.00 kV
WD = 11 mm
Signal A = SE2
Photo No. = 1120
Date :21 Jul 2008
Sample ID = CA_ J2_15 Sek. 40g / Ltr.
GKSS

Fig. 7f

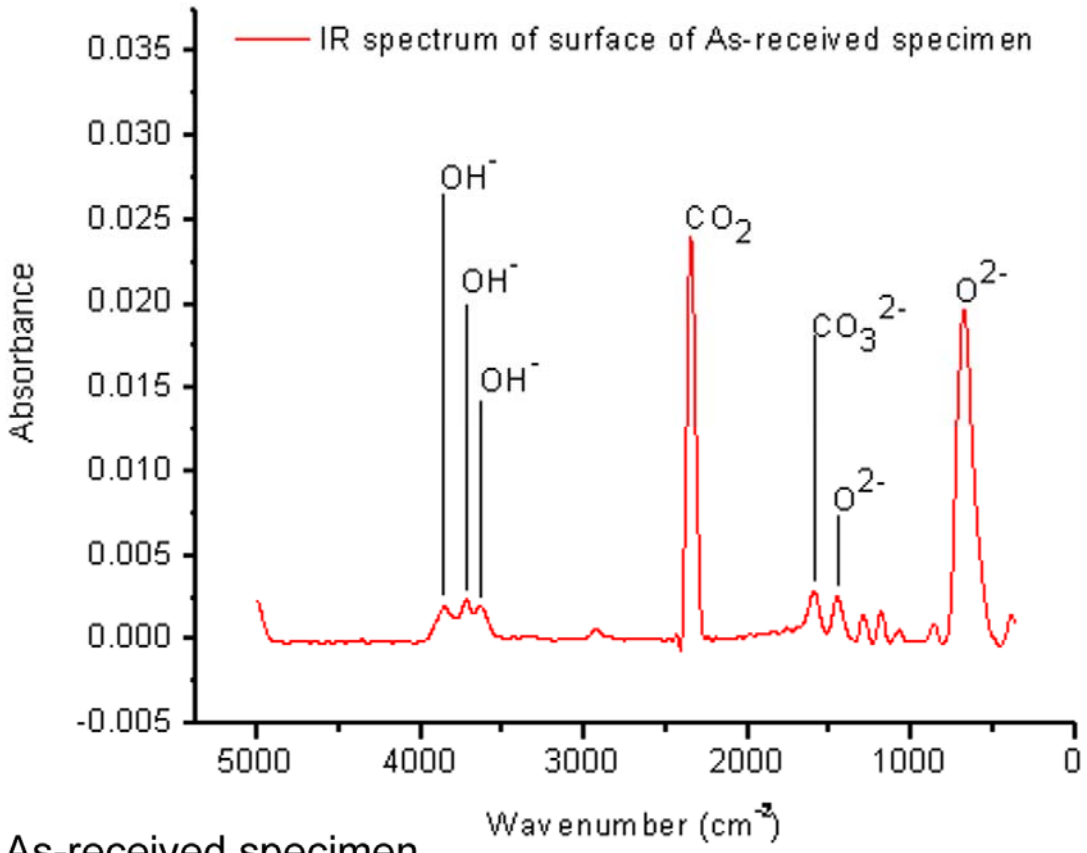

(a) As-received specimen

Fig. 8a

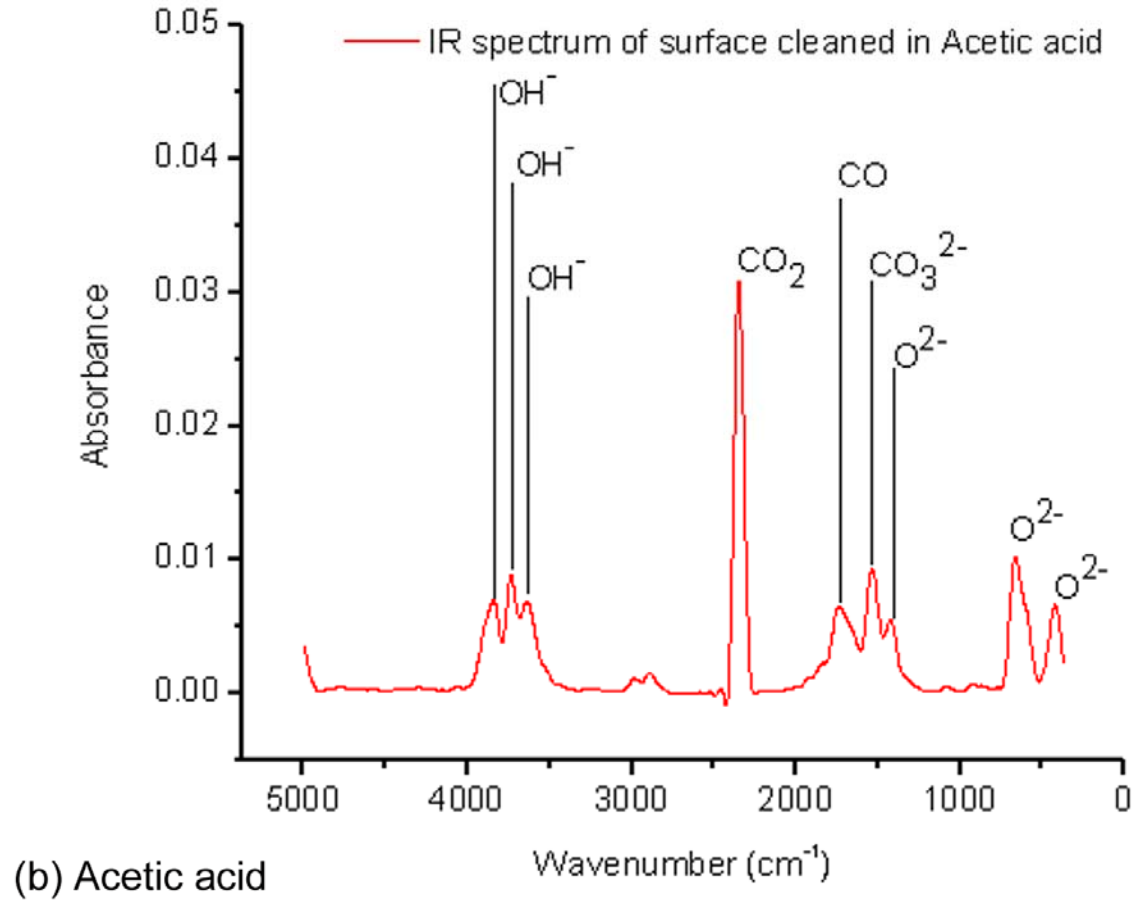

(b) Acetic acid

Fig. 8b

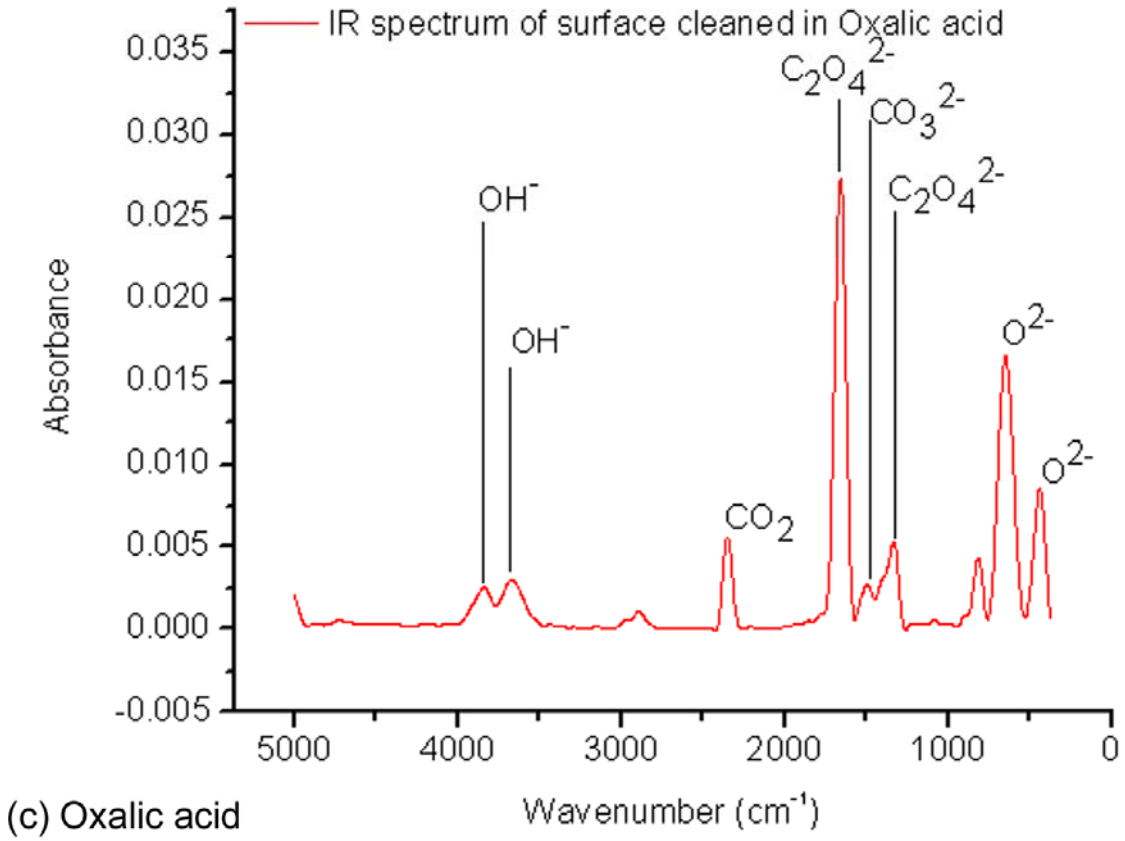

(c) Oxalic acid

Fig. 8c

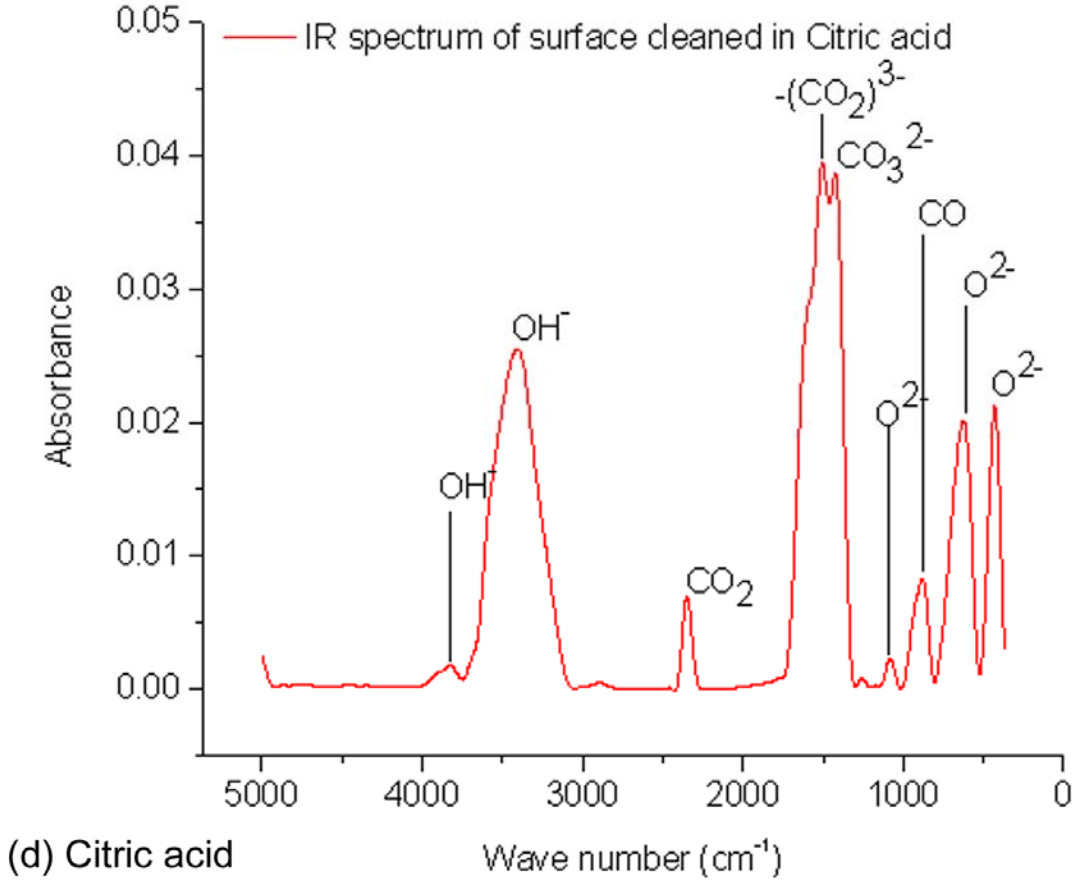

(d) Citric acid

Fig. 8d

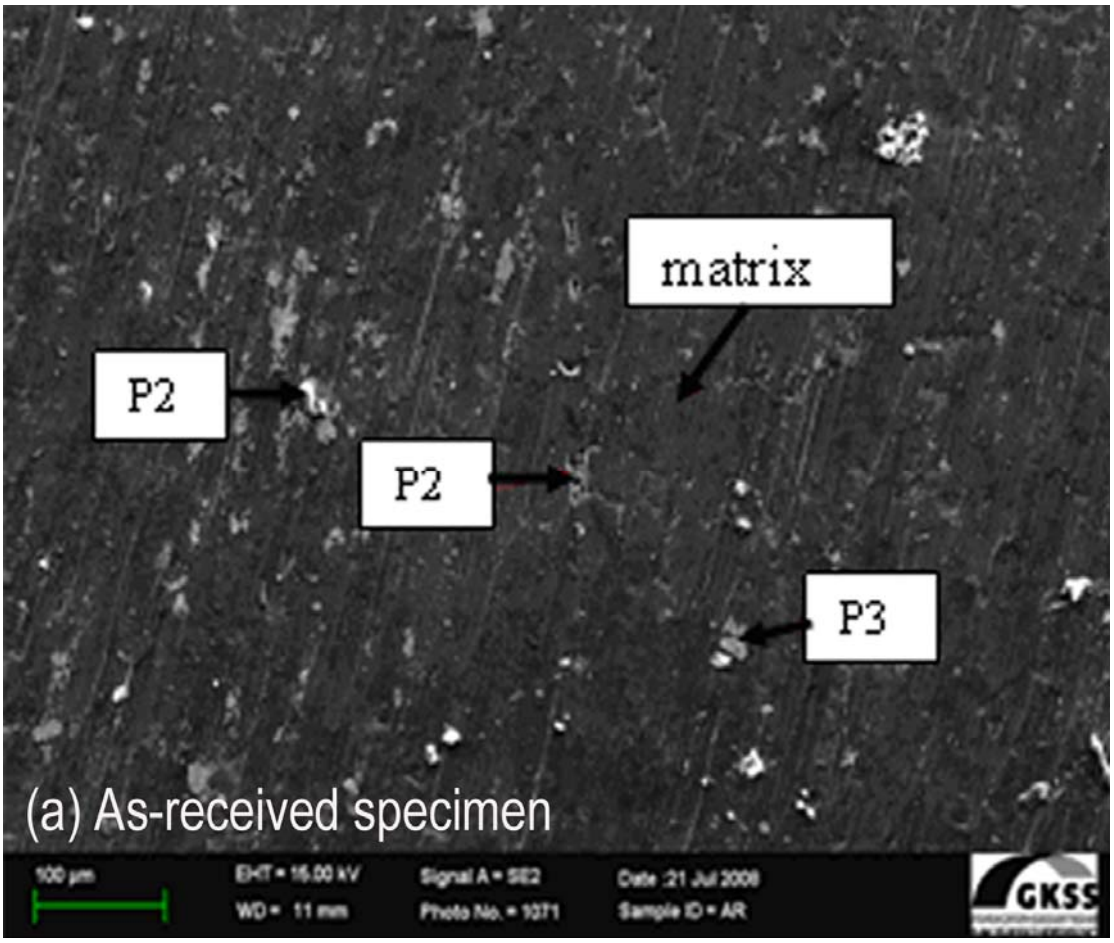
matrix
P2
P2
P3
(a) As-received specimen
100 µm
EHT = 15.00 kV
WD = 11 mm
Signal A = SE2
Photo No. = 1071
Date :21 Jul 2008
Sample ID = AR
GKSS

Fig. 9a

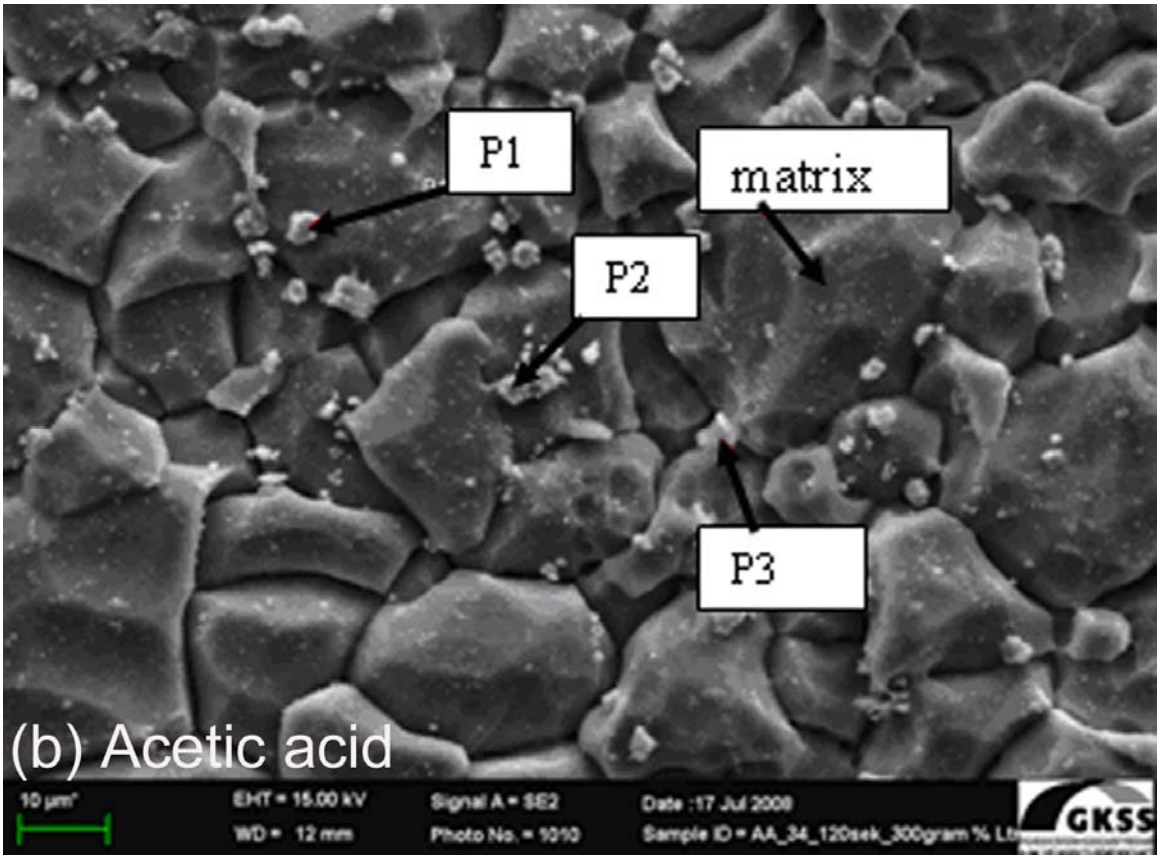
P1
matrix
P2
P3
(b) Acetic acid
10 µm
EHT = 15.00 kV
WD = 12 mm
Signal A = SE2
Photo No. = 1010
Date :17 Jul 2008
GKSS

Fig. 9b

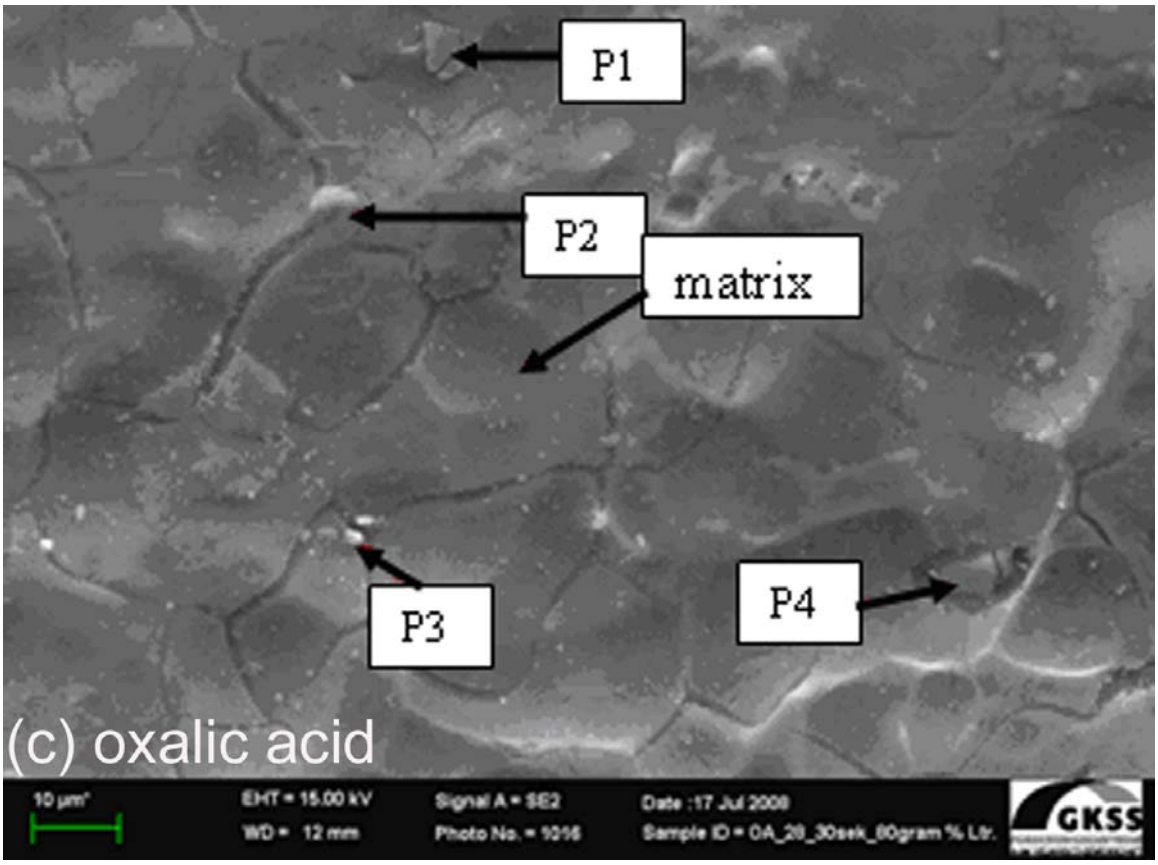
P1
P2
matrix
P3
P4
(c) oxalic acid
10 µm
EHT = 15.00 kV
WD = 12 mm
Signal A = SE2
Photo No. = 1016
Date :17 Jul 2008
Sample ID = OA_20_30sek_80gram % Ltr.
GKSS

Fig. 9c

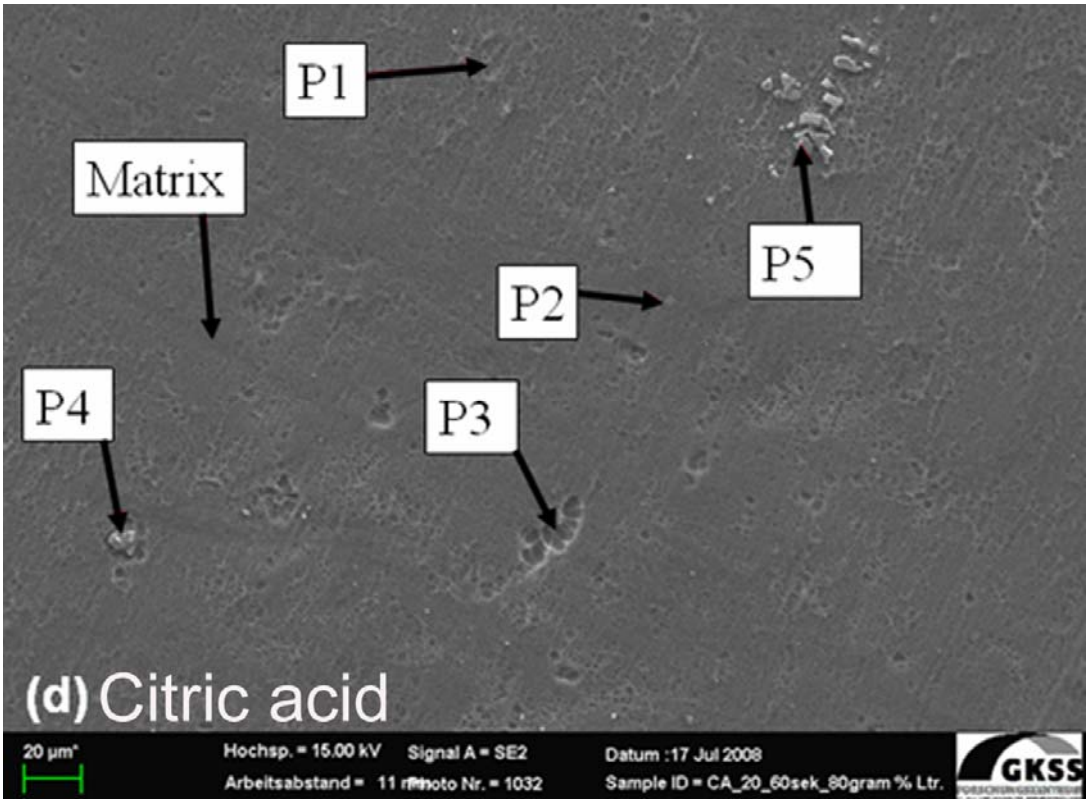
P1
Matrix
P5
P2
P4
P3
(d) Citric acid
20 µm
Hochsp. = 15.00 kV
Signal A = SE2
Datum :17 Jul 2008
Arbeitsabstand = 11 mm
Photo Nr. = 1032
Sample ID = CA_20_60sek_80gram % Ltr.
GKSS

Fig. 9d

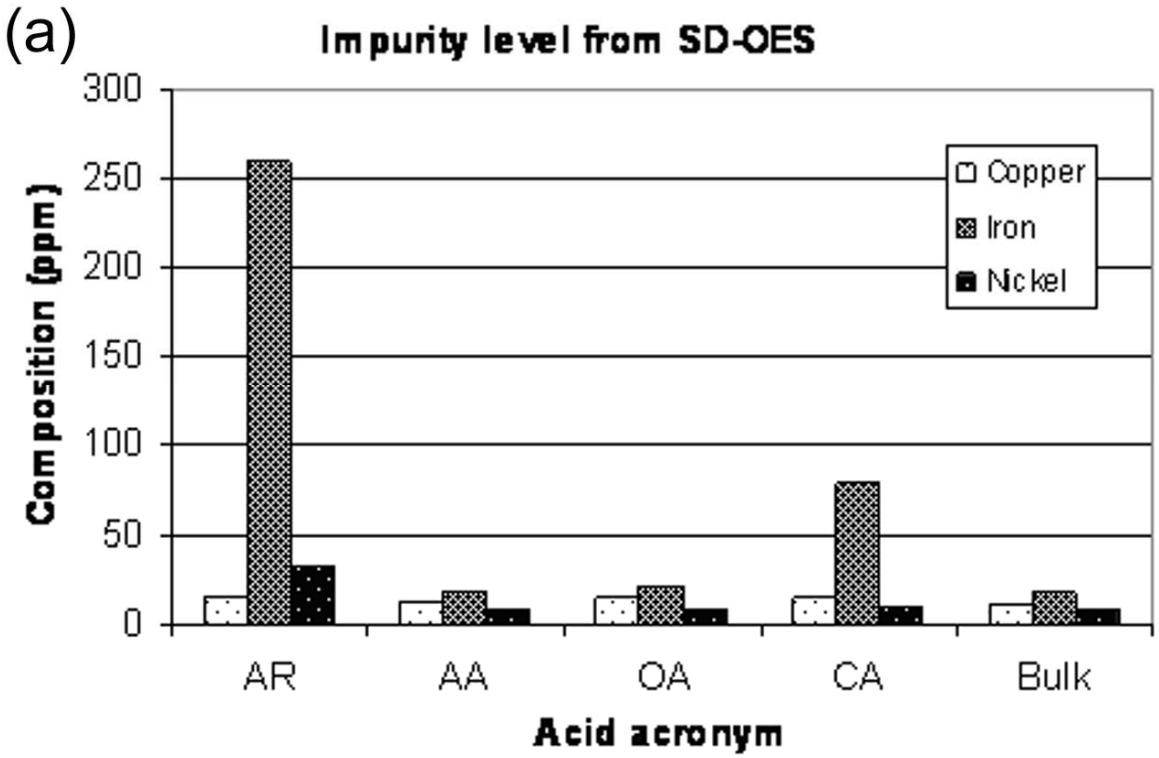
(a)
Impurity level from SD-OES
300
250
200
150
100
50
0
Composition (ppm)
Copper
Iron
Nickel
AR
AA
OA
CA
Bulk
Acid acronym

Fig. 10a

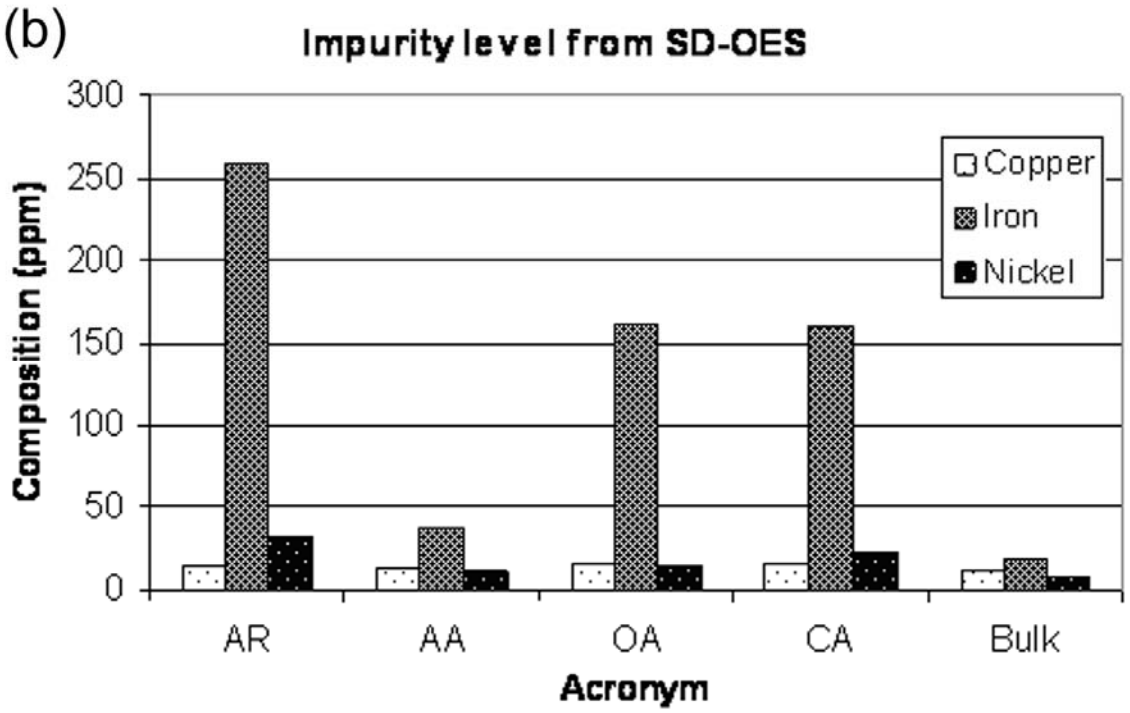
(b)
Impurity level from SD-OES
300
250
200
150
100
50
0
Composition (ppm)
Copper
Iron
Nickel
AR
AA
OA
CA
Bulk
Acronym

Fig. 10a

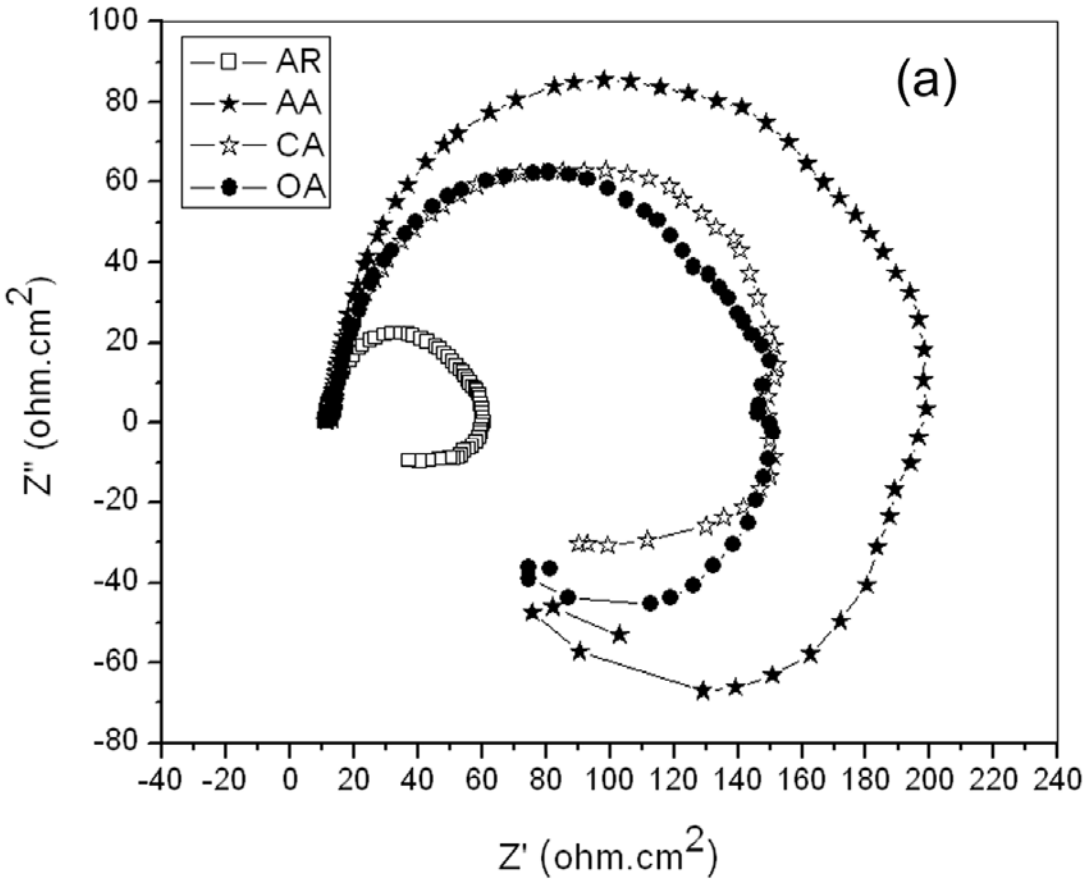
AR
AA
CA
OA
(a)
Z'' (ohm.cm2)
Z' (ohm.cm2)
100
80
60
40
20
0
-20
-40
-60
-80
-40 -20 0 20 40 60 80 100 120 140 160 180 200 220 240

Fig. 11a

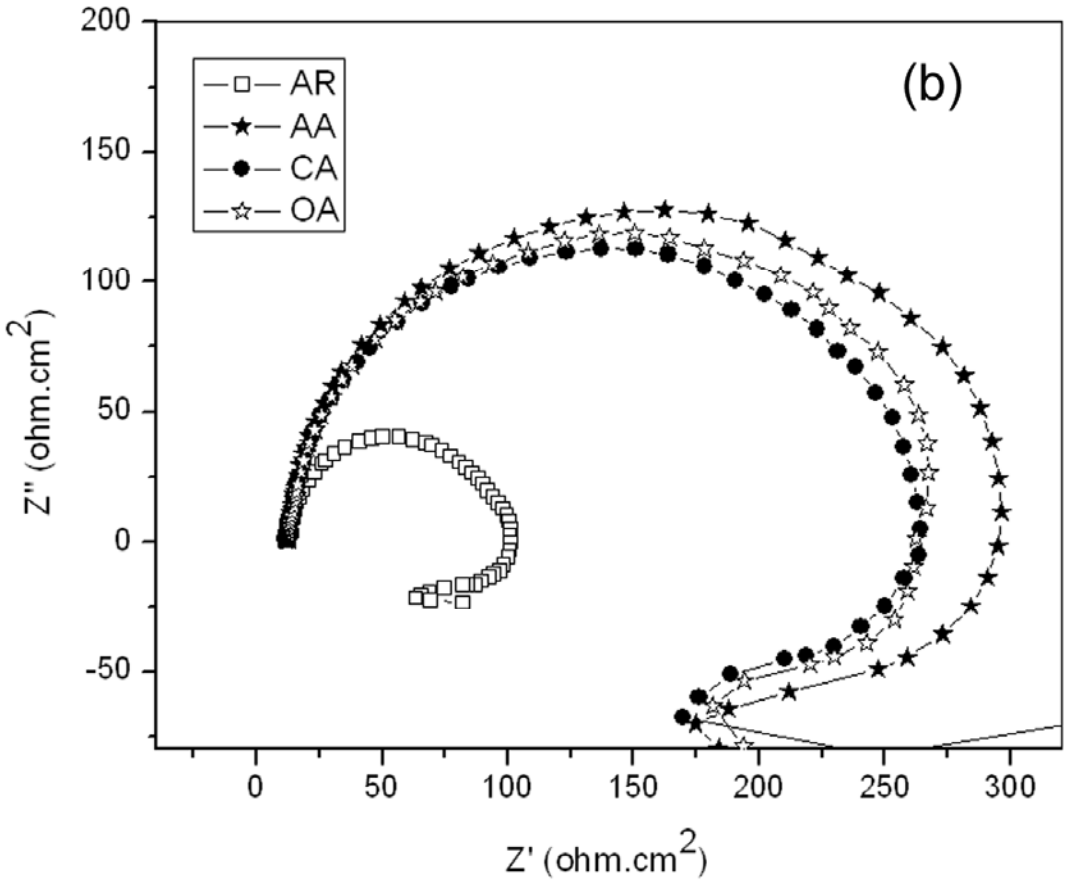
(b)
AR
AA
CA
OA
Z'' (ohm.cm2)
Z' (ohm.cm2)
200
150
100
50
0
-50
0
50
100
150
200
250
300

Fig. 11b